

TRANSVERSE FOLIATIONS IN THE ROTATING KEPLER PROBLEM

SEONGCHAN KIM

ABSTRACT. We construct finite energy foliations and transverse foliations of neighbourhoods of the circular orbits in the rotating Kepler problem for all negative energies. This paper would be a first step towards our ultimate goal that is to recover and refine McGehee's results on homoclinics [23] and to establish a theoretical foundation to the numerical demonstration of the existence of a homoclinic-heteroclinic chain in the planar circular restricted three-body problem [20], using pseudoholomorphic curves.

1. INTRODUCTION

The rotating Kepler problem is the Kepler problem in rotating coordinates, obtained from the planar circular restricted three-body problem (PCR3BP) by setting the mass of one of the primaries to zero. Its Hamiltonian $H: T^*(\mathbb{R}^2 \setminus \{0\}) \rightarrow \mathbb{R}$ is given by

$$\begin{aligned} H(q_1, q_2, p_1, p_2) &= \frac{1}{2}|p|^2 - \frac{1}{|q|} - p_2q_1 + p_1q_2 \\ &= \frac{1}{2}((p_1 + q_2)^2 + (p_2 - q_1)^2) - \frac{1}{|q|} - \frac{1}{2}|q|^2, \end{aligned} \quad (1.1)$$

where $q = (q_1, q_2)$ and $p = (p_1, p_2)$. It admits two integrals of motion

$$E = \frac{1}{2}|p|^2 - \frac{1}{|q|}, \quad L = q_1p_2 - q_2p_1, \quad (1.2)$$

called the Kepler energy and the angular momentum, respectively. Throughout the paper, we tacitly assume that the Kepler energy is negative, so that its trajectories projected to the q -plane are ellipses. We call such trajectories Kepler ellipses.

The Hamiltonian H admits a unique critical value $c = -\frac{3}{2}$. If $c < -\frac{3}{2}$, then the energy level $H^{-1}(c)$ consists of two connected components, denoted by Σ_c^b and Σ_c^u . They are called the bounded and the unbounded components, respectively. It is important to mention that the component Σ_c^b is not bounded as a set. Indeed, the point $(q_1, q_2, p_1, p_2) = (\frac{1}{a}, 0, \sqrt{2(a+c)}, 0)$ lies on Σ_c^b for any value of $a > -c$. We stick to our nomenclature though as its projection to the q -plane is bounded. If $c > -\frac{3}{2}$, then the energy level $H^{-1}(c)$ consists of a single unbounded component whose projection to the q -plane is the whole $\mathbb{R}^2 \setminus \{0\}$.

Periodic orbits will be referred to as circular orbits if the projections to the q -plane are circular. A circular orbit is called direct and retrograde if it is rotating in the same direction as the coordinate system and in opposite direction to the coordinate system, respectively. If $c < -\frac{3}{2}$, then there are precisely two circular orbits γ_{retro}^b and γ_{direct}^b on Σ_c^b and a unique circular orbit γ_{direct}^u on Σ_c^u . The circular orbit γ_{retro}^b is retrograde and the other two are direct. When $c = -\frac{3}{2}$, the two direct

circular orbits degenerate into a circle of critical points. In the case $c > -\frac{3}{2}$, there is a unique circular orbit γ_{retro}^u on $H^{-1}(c)$ that is retrograde.

Fix $c < -\frac{3}{2}$. The angular momentum L , restricted to Σ_c^b , takes values in the interval $[L_{\text{retro}}^b, L_{\text{direct}}^b]$, where $L_{\text{retro}}^b < 0$ and $L_{\text{direct}}^b > 0$ are angular momenta of γ_{retro}^b and γ_{direct}^b , respectively. See Section 3. Each $L \in (L_{\text{retro}}^b, L_{\text{direct}}^b)$ corresponds to a Liouville torus. The three-dimensional manifold Σ_c^b is not compact due to collisions. Note that along all collision orbits we have $L = 0$. However, two-body collisions can always be regularised, see for example [25, Section 2] and also [8, Section 4.1], and hence Σ_c^b can be compactified to form a closed three-dimensional manifold $\bar{\Sigma}_c^b$, diffeomorphic to $\mathbb{R}P^3$.

Consider two solid tori

$$\begin{aligned}\Sigma_{\text{retro}}^b &= \{(q, p) \in \bar{\Sigma}_c^b : (q, p) \text{ lies on an orbit with } L \in [L_{\text{retro}}^b, 0]\}, \\ \Sigma_{\text{direct}}^b &= \{(q, p) \in \bar{\Sigma}_c^b : (q, p) \text{ lies on an orbit with } L \in [0, L_{\text{direct}}^b]\}.\end{aligned}$$

Each solid torus is foliated into embedded discs, whose boundaries lie on the boundary torus consisting only of collision orbits and whose interiors are transverse to the Hamiltonian flow. The circular orbit corresponds to a unique fixed point of the associated first return map. To see this, we first note that there is a contact form on $\bar{\Sigma}_c^b$ that is dynamically convex, i.e. every contractible periodic orbit has Conley-Zehnder index at least three. See [3, Proposition 3.2] and [2, Theorem 1.1]. Then an application of a result from [17] implies that γ_{retro}^b binds a rational open book decomposition whose pages are disc-like global surfaces of section for the Hamiltonian flow. Since every $L \in [0, L_{\text{direct}}^b]$ corresponds to a Liouville torus that is tangent to the Hamiltonian flow, each of the pages of this rational open book decomposition intersects Σ_{direct}^b transversally in closed discs that determine the above-mentioned disc foliation of Σ_{direct}^b . The same holds for γ_{direct}^b and Σ_{retro}^b .

The goal of this paper is to show that similar assertions hold in neighbourhoods of γ_{direct}^u and γ_{retro}^u , as stated below.

Theorem 1.1. *The following assertions hold.*

- (1) Assume that $c < -\frac{3}{2}$. Then there is a subset Σ_{direct}^u of the unbounded component $\Sigma_c^u \subset H^{-1}(c)$ satisfying the following properties:
 - (a) It is diffeomorphic to a solid torus whose core is γ_{direct}^u and whose boundary is a Liouville torus.
 - (b) It is foliated into embedded discs whose boundaries lie on the boundary torus and whose interiors are transverse to the Hamiltonian flow.
 - (c) A unique fixed point of the associated first return map corresponds to the direct circular orbit γ_{direct}^u .
- (2) If $-\frac{3}{2} < c < 0$, then there is a subset $\Sigma_{\text{retro}}^u \subset H^{-1}(c)$ having the same properties as above, with γ_{direct}^u being replaced by γ_{retro}^u .

More precise descriptions for the subsets Σ_{direct}^u and Σ_{retro}^u in the statement above will be given in Sections 5 and 6, respectively.

Remark 1.2. Here are a couple of remarks on the theorem above.

- (1) The reason why we consider only negative energies is that we would not like to regularise the collisions. See Section 3.
- (2) The subset Σ_{direct}^u can be arbitrarily large. See Remark 5.1.

- (3) Pick any embedded disc \mathcal{D} described in (b) above. Since the rotating Kepler problem is completely integrable, the solid torus Σ_{direct}^u is foliated by Liouville tori. This Liouville foliation induces a foliation of the disc \mathcal{D} into concentric circles whose centre corresponds to the direct circular orbit γ_{direct}^u . The same holds for Σ_{retro}^u with γ_{direct}^u being replaced by γ_{retro}^u .

The motivation of this paper comes from results on the PCR3BP by McGehee [23] and by Koon, Lo, Marsden and Ross [20]. We briefly state below these results for readers' convenience.

The PCR3BP studies the motion of an infinitesimal body under the gravitational influence of two massive bodies moving along circular orbits around their center of mass. The infinitesimal body, denoted by C , is assumed to move in the plane spanned by the orbits of the two massive bodies, denoted by S and J . We rescale the total mass of the system to one, so that the mass of S equals $1 - \mu$ and the mass of J equals μ for some $\mu \in [0, 1]$. If the center of mass is located at the origin, then the Hamiltonian of the PCR3BP in a rotating frame is given by

$$H_\mu(q_1, q_2, p_1, p_2) = \frac{1}{2}|p|^2 - \frac{1 - \mu}{|q - S|} - \frac{\mu}{|q - J|} - p_2q_1 + p_1q_2,$$

where $S = (-\mu, 0)$ and $J = (1 - \mu, 0)$ denote the positions of S and J , respectively. Note that in the case $\mu = 0$, this becomes the Hamiltonian of the rotating Kepler problem, see (1.1).

We assume $\mu < \frac{1}{2}$, so that S is heavier than J . The Hamiltonian H_μ admits five equilibria $L_j, j = 1, 2, 3, 4, 5$, ordered by action in the following way:

$$H_\mu(L_1) < H_\mu(L_2) < H_\mu(L_3) < H_\mu(L_4) = H_\mu(L_5).$$

These values tend to $-\frac{3}{2}$, the critical value of the rotating Kepler problem, as $\mu \rightarrow 0$. We are interested in energies slightly above the first two critical values $H_\mu(L_1)$ and $H_\mu(L_2)$. The corresponding Hill's regions are illustrated in Figure 1. Since L_1 and

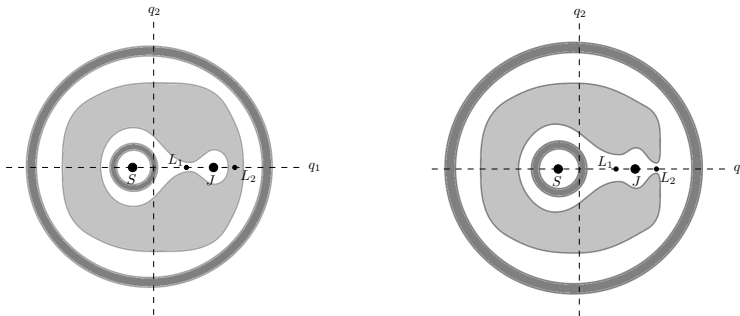


FIGURE 1. Hill's regions corresponding to energies slightly above $H_\mu(L_1)$ (left) and $H_\mu(L_2)$ (right). The darkly shaded regions indicate the projection of invariant tori.

L_2 are of saddle-center type, a theorem of Lyapunoff [21] shows that for energy slightly above $H_\mu(L_j)$, the energy level carries a unique hyperbolic periodic orbit near L_j , called the Lyapunoff orbit, $j = 1, 2$.

In his dissertation [23], McGehee established the presence of invariant tori on the energy level, as in Figure 1, for $\mu > 0$ small enough, in other words, for J

sufficiently light. By making use of these tori, he was able to find a homoclinic orbit to the Lyapunoff orbit associated with L_1 or L_2 . See Figure 2.

Using McGehee's result, Koon, Lo, Marsden and Ross provided a numerical demonstration of the existence of a homoclinic-heteroclinic chain in the Sun-Jupiter system [20]: let the mass μ of J be that of Jupiter and the energy be that of comet Oterma, so that it is slightly above $H_\mu(L_2)$. For these values, the authors showed that the energy level carries the Lyapunoff orbits near L_1 and L_2 and a heteroclinic orbit between the two Lyapunoff orbits. These three periodic orbits consist of a so-called homoclinic-heteroclinic chain, which might be used to design spacecraft orbits exploring the interior and exterior regions as illustrated in Figure 2.

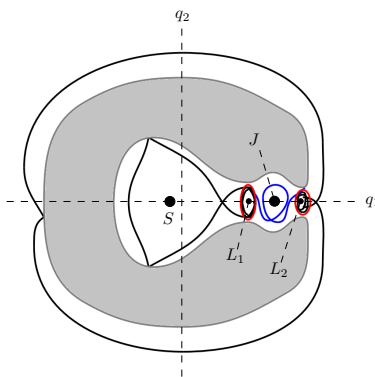


FIGURE 2. A homoclinic-heteroclinic chain in the PCR3BP. The inner and outer black curves denote homoclinic orbits to the Lyapunoff orbits (red curves) near L_1 and L_2 , respectively. The blue curve indicates a heteroclinic orbit.

Our ultimate goal is to recover and refine McGehee's results and to establish a theoretical foundation to the numerical demonstration by Koon-Lo-Marsden-Ross, using pseudoholomorphic curves. As compactness is crucial in pseudoholomorphic curve theory, in order to achieve this goal, one first has to find an efficient way to deal with non-compact energy levels. This paper would provide a way to construct finite energy foliations of regions in the non-compact energy level in the case $\mu = 0$, i.e. in the rotating Kepler problem, so it would be a first step towards our final goal.

Outline of the paper. We start by recollecting relevant facts about Reeb dynamics and pseudoholomorphic curves in symplectisations in Section 2. Then in Section 3 we review results on the rotating Kepler problem that will be needed in our argument later on. In Section 4 we recall the definition and some properties of Poincaré's coordinates, a modification of the well-known Delaunay coordinates that are not valid for the circular orbits. Constructions of finite energy foliations and transverse foliations are provided in Sections 5 and 6. We present in Appendix A an alternative way to obtain a transverse foliation whose pages are annuli.

2. BASIC NOTIONS IN CONTACT GEOMETRY

2.1. Periodic orbits. Let $\Sigma = K^{-1}(0) \subset \mathbb{R}^4$ be a regular energy level of a Hamiltonian $K: \mathbb{R}^4 \rightarrow \mathbb{R}$. We endow \mathbb{R}^4 with coordinates (x_1, x_2, y_1, y_2) . A periodic orbit

(of K) on Σ will be denoted by a pair $P = (w, T)$, where $w: \mathbb{R} \rightarrow \Sigma$ solves the differential equation $\dot{w} = X_K \circ w$, where X_K denotes the Hamiltonian vector field of K , defined as $\omega_0(X_K, \cdot) = -dK$, and $T > 0$ is a period. Here, $\omega_0 = dy_1 \wedge dx_1 + dy_2 \wedge dx_2$ denotes the standard symplectic form on \mathbb{R}^4 . By abuse of notation, we may also denote by P the trace $w(\mathbb{R}) \subset \Sigma$. If T is minimal, then P is called simple. Throughout the paper, when we consider a periodic orbit, then we tacitly assume that it is simple. If two periodic orbits $P_1 = (w_1, T_1)$ and $P_2 = (w_2, T_2)$ satisfy $w_1(\mathbb{R}) = w_2(\mathbb{R})$ and $T_1 = T_2$, then they are identified, and we write $P_1 = P_2$.

Suppose that K is invariant under an anti-symplectic involution $\rho: \mathbb{R}^4 \rightarrow \mathbb{R}^4$, meaning that ρ is an involution satisfying $\rho^*\omega_0 = -\omega_0$. The Hamiltonian vector field satisfies $\rho_*X_K = -X_K$, so that

$$\phi_K^t = \rho \circ \phi_K^{-t} \circ \rho,$$

where ϕ_K^t indicates the flow of X_K , called the Hamiltonian flow of K . This shows that if $P = (w, T)$ is a periodic orbit, then $P_\rho = (w_\rho, T)$, defined as

$$w_\rho: \mathbb{R} \rightarrow \Sigma, \quad w_\rho(t) = \rho \circ w(T - t),$$

is a periodic orbit as well. In the case that $w(\mathbb{R}) = w_\rho(\mathbb{R})$, we write $P = P_\rho$ and call it a symmetric periodic orbit (with respect to ρ). Note that every symmetric periodic orbit intersects the fixed point set $\text{Fix}(\rho)$, which is assumed to be non-empty, precisely at two points.

Assume that Σ is compact and of contact type, i.e. there is a Liouville vector field Y that is transverse to Σ . The one-form $\lambda = \omega_0(Y, \cdot)$ restricts to a contact form on Σ , still denoted by λ . Denote by $R = R_\lambda$ the Reeb vector field of λ . Note that the Hamiltonian vector field X_K and the Reeb vector field R are related by

$$R = \frac{1}{\lambda(X_K)} X_K,$$

implying that their flows coincide up to reparametrisation. The Reeb period of a periodic orbit P is defined as the period of P with respect to the Reeb flow.

If the Liouville vector field Y is invariant under ρ , i.e. it satisfies $\rho_*Y = Y$, then ρ becomes exact, meaning that it satisfies $\rho^*\lambda = -\lambda$. In this case, ρ restricts to an anti-contact involution on the contact manifold (Σ, λ) , again denoted by ρ . The triple (Σ, λ, ρ) is said to be a real contact manifold. Note that the Reeb vector field R and the Reeb flow ϕ_R^t satisfy

$$\rho_*R = -R, \quad \phi_R^t = \rho \circ \phi_R^{-t} \circ \rho.$$

Therefore, given a periodic orbit $P = (w, T)$, the Reeb periods of P and P_ρ coincide.

2.2. Conley-Zehnder index. As before, let $\Sigma = K^{-1}(0) \subset \mathbb{R}^4$ be a compact energy level of $K: \mathbb{R}^4 \rightarrow \mathbb{R}$, equipped with a transverse Liouville vector field Y . The corresponding contact form is denoted again by λ .

For every $z = (x_1, x_2, y_1, y_2) \in \Sigma$ the tangent space $T_z\Sigma$ is spanned by the orthogonal vectors X_1, X_2, X_3 , defined as

$$X_j = A_j \nabla K, \quad j = 1, 2, 3, \tag{2.1}$$

where the 4×4 matrices $A_j, j = 1, 2, 3$, are given by

$$A_1 = \begin{pmatrix} 0 & J \\ J & 0 \end{pmatrix}, \quad A_2 = \begin{pmatrix} J & 0 \\ 0 & -J \end{pmatrix}, \quad A_3 = \begin{pmatrix} 0 & I \\ -I & 0 \end{pmatrix},$$

with

$$I = \begin{pmatrix} 1 & 0 \\ 0 & 1 \end{pmatrix}, \quad J = \begin{pmatrix} 0 & 1 \\ -1 & 0 \end{pmatrix}.$$

Note that $X_3 = A_3 \nabla K = X_K$ is parallel to the Reeb vector field R . The projection $\pi: T\Sigma \rightarrow \xi = \ker \lambda$ along R restricted to the tangent plane distribution $\text{span}\{X_1, X_2\}$ induces an isomorphism from $\text{span}\{X_1, X_2\}$ to the contact structure ξ . In particular, the latter is spanned by the vector fields

$$\begin{aligned} \bar{X}_1 &= \pi(X_1) = X_1 - \lambda(X_1)R, \\ \bar{X}_2 &= \pi(X_2) = X_2 - \lambda(X_2)R. \end{aligned} \tag{2.2}$$

Let \mathfrak{T} denote the unitary trivialisation of $T\Sigma/\mathbb{R}X_3$, induced by X_1 and X_2 . Set

$$\kappa_{ij} := \langle \text{Hess}K \cdot X_i, X_j \rangle, \quad i, j = 1, 2, 3.$$

In the trivialisation \mathfrak{T} the transverse linearised flow of the Hamiltonian vector field X_K along a periodic trajectory $P = (w, T)$ on Σ is described by solutions $\alpha(t) = (\alpha_1(t), \alpha_2(t)) \in \mathbb{R}^2$ to the ODE

$$\begin{pmatrix} \dot{\alpha}_1(t) \\ \dot{\alpha}_2(t) \end{pmatrix} = \begin{pmatrix} -\kappa_{12} & -\kappa_{22} - \kappa_{33} \\ \kappa_{11} + \kappa_{33} & \kappa_{12} \end{pmatrix} \Big|_{w(t)} \begin{pmatrix} \alpha_1(t) \\ \alpha_2(t) \end{pmatrix}. \tag{2.3}$$

Let $\vartheta(t)$ be any continuous argument of a non-vanishing solution $\alpha(t)$, i.e. $\alpha_1(t) + i\alpha_2(t) \in \mathbb{R}_+ e^{i\vartheta(t)}$. Define the rotation interval of P as

$$I = \{\vartheta(T) - \vartheta(0) \mid \alpha(0) \neq 0\}, \tag{2.4}$$

which depends only on the initial condition $\alpha(0) \neq 0$. It is a compact connected interval with length strictly less than π . The periodic orbit P is non-degenerate if and only if $\partial I \cap 2\pi\mathbb{Z} = \emptyset$. Given $\varepsilon > 0$ small enough, we set $I_\varepsilon := I - \varepsilon$. Then the Conley-Zehnder index of P is defined as

$$\mu_{\text{CZ}}(P) = \begin{cases} 2k + 1 & \text{if } I_\varepsilon \subset (2k\pi, 2(k+1)\pi), \\ 2k & \text{if } 2k\pi \in \text{int}(I_\varepsilon). \end{cases}$$

Note that in this definition the Conley-Zehnder index is lower semi-continuous with respect to the C^0 -topology.

Suppose that the Hamiltonian K is invariant under an anti-symplectic involution $\rho: \mathbb{R}^4 \rightarrow \mathbb{R}^4$, and the Liouville vector field Y satisfies $\rho_* Y = Y$, so that ρ restricts to an anti-contact involution of Σ , denoted again by ρ , as in the previous section. Since

$$\rho_* X_j = X_j, \quad j = 1, 2, 3,$$

we find by the definition of the Conley-Zehnder index that

$$\mu_{\text{CZ}}(P_\rho) = \mu_{\text{CZ}}(P).$$

2.3. Pseudoholomorphic curves in symplectisations. Let (Σ, λ) be a closed contact three-manifold. We denote by $\mathcal{J}(\lambda)$ the set of $d\lambda$ -compatible almost complex structures on $\xi = \ker \lambda$. We extend each $J \in \mathcal{J}(\lambda)$ to a $d(e^r \lambda)$ -compatible almost complex structure \tilde{J} on $T(\mathbb{R} \times \Sigma)$ that is given by

$$\tilde{J}: \partial_r \mapsto R, \quad \tilde{J}|_\xi = J, \tag{2.5}$$

where r denotes the coordinate on \mathbb{R} . Note that \tilde{J} is \mathbb{R} -invariant.

Given a closed Riemann surface (S, j) and a finite set $\Gamma \subset S$, we consider a smooth map $\tilde{u} = (a, u): S \setminus \Gamma \rightarrow \mathbb{R} \times \Sigma$, satisfying $d\tilde{u} \circ j = \tilde{J} \circ d\tilde{u}$ and a finite energy condition

$$0 < E(\tilde{u}) := \sup_{\phi} \int_{S \setminus \Gamma} \tilde{u}^* d(\phi\lambda) < \infty,$$

where the supremum is taken over all monotone increasing smooth functions $\phi: \mathbb{R} \rightarrow [0, 1]$. In this paper we only consider the case $S = S^2$ and $\#\Gamma \in \{1, 2\}$. If $\#\Gamma = 1$ or $\#\Gamma = 2$, then such a map is called a finite energy plane or a finite energy cylinder, respectively.

Points in Γ are called punctures of $\tilde{u} = (a, u)$. If a is bounded in a small neighbourhood of a puncture $z_0 \in \Gamma$, then z_0 is called removable. In this case, \tilde{u} can be smoothly extended over z_0 . See [9]. Otherwise, either $a(z) \rightarrow +\infty$ or $a(z) \rightarrow -\infty$ as $z \rightarrow z_0$. Then the puncture z_0 is called positive or negative, respectively. In the following we assume that every puncture is not removable, so that the set Γ is decomposed into $\Gamma = \Gamma^+ \sqcup \Gamma^-$, where Γ^\pm consist only of positive/negative punctures, respectively. We assign $\varepsilon \in \{\pm 1\}$ to each puncture $z_0 \in \Gamma^\pm$ according to its sign.

The following statement is taken from [9] and [11].

Theorem 2.1. *Given $z_0 \in \Gamma$ choose a holomorphic chart $\varphi: (\mathbb{D} \setminus \partial\mathbb{D}, 0) \rightarrow (\varphi(\mathbb{D} \setminus \partial\mathbb{D}), z_0)$ centred at z_0 . Abbreviate $\tilde{u}(s, t) = \tilde{u} \circ \varphi(e^{-2\pi(s+it)})$, $(s, t) \in [0, +\infty) \times \mathbb{R}/\mathbb{Z}$. Then every sequence $s_n \rightarrow +\infty$ admits a subsequence s_{n_k} and a τ -periodic orbit x of the Reeb vector field such that $u(s_{n_k}, t) \rightarrow x(\varepsilon\tau t + d)$ in $C^\infty(\mathbb{R}/\mathbb{Z}, \Sigma)$ as $k \rightarrow +\infty$, for some $d \in \mathbb{R}$. In the case x is non-degenerate, $u(s, t) \rightarrow x(\varepsilon\tau t + d)$ in $C^\infty(\mathbb{R}/\mathbb{Z}, \Sigma)$ as $s \rightarrow +\infty$.*

The periodic orbit x in the theorem above is called an asymptotic limit of \tilde{u} at the puncture $z_0 \in \Gamma$. If the puncture z_0 is positive or negative, the corresponding asymptotic limit is also called positive or negative, respectively. A finite energy curve is called non-degenerate if its every asymptotic limit is non-degenerate. The theorem above shows that a non-degenerate finite energy plane admits a unique asymptotic limit.

We now assume that (Σ, λ) is equipped with an anti-contact involution ρ . It defines the exact anti-symplectic involution $\tilde{\rho} := \text{Id}_{\mathbb{R}} \times \rho$ on $(\mathbb{R} \times \Sigma, d(e^r \lambda))$, meaning that $\tilde{\rho}^*(e^r \lambda) = -e^r \lambda$. An almost complex structure $J \in \mathcal{J}(\lambda)$ is said to be ρ -anti-invariant if

$$D\rho|_{\xi} \circ J \circ (D\rho|_{\xi})^{-1} = -J. \quad (2.6)$$

Denote by $\mathcal{J}_\rho(\lambda) \subset \mathcal{J}(\lambda)$ the set of $d\lambda$ -compatible and ρ -anti-invariant almost complex structures on ξ . If $J \in \mathcal{J}_\rho(\lambda)$, then the associated $d(e^r \lambda)$ -compatible almost complex structure \tilde{J} as in (2.5) is $\tilde{\rho}$ -anti-invariant. It follows that if $\tilde{u} = (a, u)$ is a finite energy \tilde{J} -holomorphic curve, then $\tilde{u}_\rho := \rho \circ \tilde{u} \circ I$, where $I(z) = \bar{z}$, is a finite energy \tilde{J} -holomorphic curve with Hofer energy $E(\tilde{u}_\rho) = E(\tilde{u})$. Moreover, if x is a positive or negative asymptotic limit of \tilde{u} at $z_0 \in \Gamma$, then x_ρ is a positive or negative asymptotic limit of \tilde{u}_ρ at $\bar{z}_0 \in I(\Gamma)$, respectively. If $\tilde{u} = \tilde{u}_\rho$, then it is said to be invariant (with respect to ρ). Note that every asymptotic limit of invariant finite energy planes and cylinders has to be a symmetric periodic orbit. For more information on the behaviour of pseudoholomorphic curves under the symmetry, we refer the reader to [7, 19].

2.4. Transverse foliations. Let ψ^t be a smooth flow on an oriented closed three-manifold Σ . A transverse foliation \mathcal{F} of Σ adapted to ψ^t is formed by the following data:

- (1) the singular set \mathcal{P} which consists of finitely many simple periodic orbits, called binding orbits.
- (2) a smooth foliation of $\Sigma \setminus \bigcup_{P \in \mathcal{P}} P$ by properly embedded surfaces transverse to the flow. Each leaf $\mathring{F} \in \mathcal{F}$ has an orientation induced by the flow and the orientation of Σ . The closure F of \mathring{F} is a compact embedded surface in Σ whose boundary is a subset of \mathcal{P} . Each end z of \mathring{F} is called a puncture. Every puncture z is associated with a binding orbit $P_z \in \mathcal{P}$, called the asymptotic limit of \mathring{F} at z . The asymptotic limit P_z at z has two orientations, one induced by \mathring{F} and the other induced by the flow. If the two orientations coincide with each other, then the puncture z is said to be positive. Otherwise it is negative.

In the case where Σ has a non-empty boundary that is tangent to the flow, then we extend the definition of a transverse foliation in such a way that every binding orbit is required to be contained in the interior of Σ and each regular leaf is transverse to the boundary of Σ .

Assume that the flow ψ^t is anti-invariant under a smooth involution $\rho: \Sigma \rightarrow \Sigma$, meaning that $\psi^t = \rho \circ \psi^{-t} \circ \rho$. A transverse foliation \mathcal{F} is said to be symmetric (with respect to ρ) if $P_\rho \in \mathcal{P}$, $\forall P \in \mathcal{P}$, and $F_\rho := \rho(\mathring{F}) \in \mathcal{F}$, $\forall \mathring{F} \in \mathcal{F}$.

2.5. Finite energy foliations. Let λ be a contact form on the tight three-sphere (S^3, ξ_0) and $J \in \mathcal{J}(\lambda)$.

Definition 2.2. A (stable) finite energy foliation for (S^3, λ, J) is a two-dimensional smooth foliation $\tilde{\mathcal{F}}$ of $\mathbb{R} \times S^3$ satisfying the following properties:

- (1) Every leaf $\tilde{F} \in \tilde{\mathcal{F}}$ is the image of an embedded finite energy \tilde{J} -holomorphic curve $\tilde{u}_{\tilde{F}} = (a_{\tilde{F}}, u_{\tilde{F}})$ having only one positive puncture. The number of negative punctures is any finite number. The energies of such finite energy surfaces are uniformly bounded.
- (2) Every asymptotic limit of \tilde{F} is unknotted and has Conley-Zehnder index 1, 2 or 3, where asymptotic limits of a leaf \tilde{F} is defined to be asymptotic limits of $\tilde{u}_{\tilde{F}}$.
- (3) A map $T: \mathbb{R} \times \tilde{\mathcal{F}} \rightarrow \tilde{\mathcal{F}}$,

$$T(c, \tilde{F}) = \{(c + a, z) \in \mathbb{R} \times S^3 \mid (a, z) \in \tilde{F}\},$$

defines an \mathbb{R} -action on $\tilde{\mathcal{F}}$. If \tilde{F} is a fixed point of T , i.e. $T(c, \tilde{F}) = \tilde{F}$, $\forall c \in \mathbb{R}$, then its Fredholm index $\text{Ind}(\tilde{F}) := \text{Ind}(\tilde{u}_{\tilde{F}})$ is equal to 0 and $\tilde{u}_{\tilde{F}}$ is a cylinder over a periodic orbit. Here, the Fredholm index $\text{Ind}(\tilde{u}_{\tilde{F}})$ represents the local dimension of the moduli space of unparametrised \tilde{J} -holomorphic curves near $\tilde{u}_{\tilde{F}}$ having the same asymptotic limits. In the case \tilde{F} is not a fixed point, then $\text{Ind}(\tilde{F}) \in \{1, 2\}$ and $u_{\tilde{F}}$ is embedded and transverse to the Reeb flow of λ .

Every non-degenerate contact form λ admits a finite energy foliation, as stated below.

Theorem 2.3 (Hofer, Wysocki and Zehnder [14]). *Let λ be a non-degenerate contact form on (S^3, ξ_0) . Then for a generic J , there is a finite energy foliation for (S^3, λ, J) .*

The projection of a finite energy foliation, obtained in the theorem above, to S^3 provides a transverse foliation adapted to the Reeb flow of λ .

Suppose that (S^3, λ) admits an anti-contact involution ρ and that $J \in \mathcal{J}_\rho(\lambda)$. A finite energy foliation $\tilde{\mathcal{F}}$ is said to be symmetric (with respect to ρ) if $\tilde{\rho}(\tilde{\mathcal{F}}) = \tilde{\mathcal{F}}$. The projection of a symmetric finite energy foliation to S^3 produces a symmetric transverse foliation.

3. THE ROTATING KEPLER PROBLEM

Recall that the Hamiltonian of the rotating Kepler problem is given by

$$H(q_1, q_2, p_1, p_2) = \frac{1}{2}((p_1 + q_2)^2 + (p_2 - q_1)^2) - \frac{1}{|q|} - \frac{1}{2}|q|^2.$$

Consider a smooth function

$$f(r) = -\frac{1}{r} - \frac{1}{2}r^2, \quad r > 0.$$

It is strictly increasing for $r < 1$ and decreasing for $r > 1$ and attains a unique global maximum $-\frac{3}{2}$ at $r = 1$. Therefore, for every $c < -\frac{3}{2}$ the equation $f(r) = c$ has precisely two roots $r_c^b < 1 < r_c^u$. It follows that for every $c < -\frac{3}{2}$ the energy level $H^{-1}(c)$ consists of two components, Σ_c^b that projects to $\{q \in \mathbb{R}^2 \setminus \{0\} : |q| \leq r_c^b\}$ and Σ_c^u that projects to $\{q \in \mathbb{R}^2 \setminus \{0\} : |q| \geq r_c^u\}$. If $-\frac{3}{2} < c < 0$, then $H^{-1}(c)$ is connected and projects to $\mathbb{R}^2 \setminus \{0\}$.

Since $\{E, L\} = 0$, where the Kepler energy E and the angular momentum L are as in (1.2), the Hamiltonian flows of E and L commute:

$$\phi_H^t = \phi_{E-L}^t = \phi_E^t \circ \phi_{-L}^t = \phi_{-L}^t \circ \phi_E^t = \phi_L^{-t} \circ \phi_E^t.$$

See, for instance, [8, Theorem 3.1.7]. Therefore, given a trajectory $\gamma(t)$ of H , i.e. a trajectory of the Hamiltonian vector field X_H , there exists a Kepler ellipse $\alpha(t)$ such that

$$\gamma(t) = \exp(-it)\alpha(t). \quad (3.1)$$

Note that γ is not necessarily periodic. It is periodic if and only if the period of α and 2π are \mathbb{Q} -commensurable. In other words, if we denote the period of α by $T > 0$, then γ is periodic if and only if

$$kT = 2\pi l \quad \text{for some coprime positive integers } k, l. \quad (3.2)$$

Let $\alpha(t)$ be a Kepler ellipse that projects to a circular orbit. Then $\gamma(t)$, as in (3.1), is circular as well. This happens if and only if X_E and X_L are parallel along $\alpha(t)$. In order to study circular orbits, recall that the eccentricity e of a Kepler ellipse satisfies

$$e^2 = 2EL^2 + 1. \quad (3.3)$$

Since circular orbits have $e = 0$, we obtain

$$0 = 2E(H - E)^2 + 1. \quad (3.4)$$

Fix $H = c$. If $c < -\frac{3}{2}$, then equation (3.4) has three solutions

$$E_{\text{retro}}^b < E_{\text{direct}}^b < -\frac{1}{2} < E_{\text{direct}}^u < 0,$$

implying that $H^{-1}(c)$ carries precisely three circular orbits: γ_{retro}^b with $E = E_{\text{retro}}^b$ and γ_{direct}^b with $E = E_{\text{direct}}^b$, both lying on Σ_c^b , and γ_{direct}^u with $E = E_{\text{direct}}^u$, lying on Σ_c^u . Their angular momenta are

$$L_{\text{retro}}^b = -\frac{1}{\sqrt{-2E_{\text{retro}}^b}}, \quad L_{\text{direct}}^b = \frac{1}{\sqrt{-2E_{\text{direct}}^b}}, \quad L_{\text{direct}}^u = \frac{1}{\sqrt{-2E_{\text{direct}}^u}},$$

respectively. Note that our coordinate system rotates in the counterclockwise direction. Therefore, γ_{retro}^b rotates in opposite direction to the coordinate system and γ_{direct}^b and γ_{direct}^u rotate in the same direction with the coordinate system. For this reason, γ_{retro}^b is called the retrograde circular orbit and γ_{direct}^b and γ_{direct}^u are called the direct circular orbits.

Assume that $-\frac{3}{2} < c < 0$. In this case, equation (3.4) has a unique solution $E = E_{\text{retro}}^u \in (-2, 0)$, implying that $H^{-1}(c)$ carries a unique circular orbit, denoted by γ_{retro}^u , whose angular momentum is given by

$$L_{\text{retro}}^u = -\frac{1}{\sqrt{-2E_{\text{retro}}^u}} \in \left(-\frac{1}{\sqrt{3/2}}, -\frac{1}{2}\right).$$

This unique circular orbit is retrograde. See Figure 3.

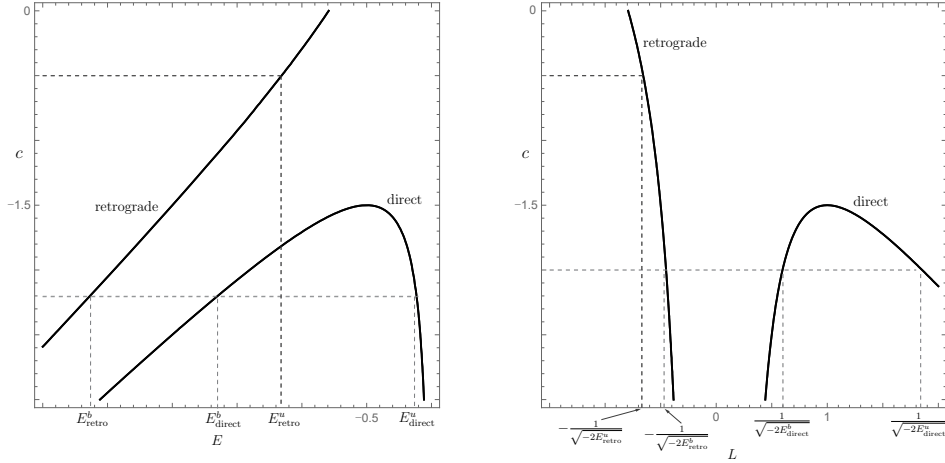


FIGURE 3. The solution set of (left) $2E(c - E)^2 + 1 = 0$; (right) $2(c + L)L^2 + 1 = 0$ is the union of two graphs. The left and right curves indicate the retrograde and direct circular orbits, respectively.

Suppose that $\alpha(t)$ is a non-circular Kepler ellipse and let $\gamma(t)$ be the corresponding periodic trajectory of H , satisfying (3.1) and (3.2). Since L generates rotation, it implies that $\gamma(t)$ lies in an S^1 -family of periodic trajectories of H satisfying the same condition. For this reason we call a periodic trajectory of H satisfying (3.2) a $T_{k,l}$ -type orbit and an S^1 -family of $T_{k,l}$ -type orbits a $T_{k,l}$ -torus.

The Kepler energy is constant along each $T_{k,l}$ -torus. Indeed, Kepler's third law implies

$$T^2 = \frac{(2\pi)^2}{(-2E)^3},$$

and hence using (3.2) we obtain

$$E_{k,l} := -\frac{1}{2} \left(\frac{k}{l} \right)^{\frac{2}{3}}.$$

One can easily check that in the case $c < -\frac{3}{2}$ all $T_{k,l}$ -type orbits satisfy $k > l$ on Σ_c^b and $k < l$ on Σ_c^u .

For a fixed coprime $k, l \in \mathbb{N}$, identity (3.3) determines a one-parameter family of $T_{k,l}$ -tori. Either the eccentricity e , the angular momentum L or the total energy $H = c$ can be regarded as the parameter of such a family. We call this family the $T_{k,l}$ -torus family. See Figure 4.

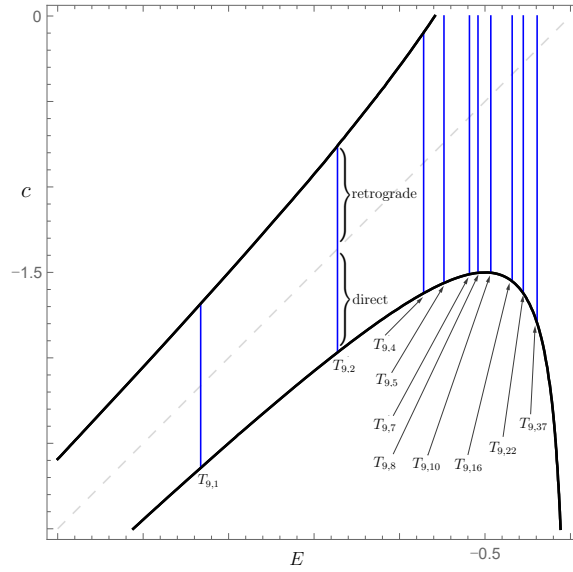


FIGURE 4. Some $T_{k,l}$ -tori with $k = 9$. The dashed line indicates the tori consisting only of collision orbits.

Observe that along every $T_{k,l}$ -torus family, there is a unique $T_{k,l}$ -torus containing a collision orbit (and hence it consists only of collision orbits). Indeed, a $T_{k,l}$ -type orbit $\gamma(t)$ is a collision orbit if and only if a Kepler ellipse $\alpha(t)$ is a collision orbit. This happens precisely at $e = 1$, and in view of (3.3) this implies $L = 0$, or equivalently $H = E$. A $T_{k,l}$ -type orbit is said to be direct or retrograde if it satisfies $L > 0$ or $L < 0$, respectively.

We summarize the discussion so far in the following. Recall that we consider orbits with $E < 0$.

Lemma 3.1. *Let $c < -\frac{3}{2}$. When projected to Σ_c^b , the Kepler energy E satisfies*

$$E_{\text{retro}}^b \leq E \leq E_{\text{direct}}^b < -\frac{1}{2}$$

and the angular momentum L satisfies

$$L_{\text{retro}}^b \leq L \leq L_{\text{direct}}^b < 1.$$

When projected to Σ_c^u , we have

$$-\frac{1}{2} < E_{\text{direct}}^u \leq E < 0, \quad 1 < L_{\text{direct}}^u \leq L < -c.$$

In the case $-\frac{3}{2} < c < 0$, we have

$$-2 < E_{\text{retro}}^u \leq E < 0, \quad -\frac{1}{\sqrt[3]{2}} < L_{\text{retro}}^u \leq L < -c.$$

4. POINCARÉ'S COORDINATES

We briefly recall the definition of Poincaré's coordinates. For more details we refer the reader to [1, Chapter 9] and [24, Section 8.9].

Consider the following open subset of $T^*(\mathbb{R}^2 \setminus \{0\})$

$$\mathcal{E} = \{(q, p) \in T^*(\mathbb{R}^2 \setminus \{0\}) : E(q, p) < 0 < e(q, p) < 1, L(q, p) > 0\},$$

called the direct elliptical domain (recall that we have $L > 0$ along direct orbits, see Section 3), and define smooth maps $\alpha, \beta: \mathcal{E} \rightarrow \mathbb{R}/2\pi\mathbb{Z}$ and $a: \mathcal{E} \rightarrow \mathbb{R}$ as follows. Choose $(q, p) \in \mathcal{E}$ and let γ denote the Kepler ellipse on which the point (q, p) lies. Then $\alpha = \alpha(q, p)$ is defined as the argument of the position q , and $\beta = \beta(q, p)$ is defined to be the argument of the perihelion, i.e. the point, lying on the projection of γ to the q -plane, that is nearest to the origin. Finally, $a = a(q, p)$ is defined to be the semi-major axis of the Kepler ellipse γ . Note that $a = -\frac{1}{2E}$, where $E < 0$ indicates the Kepler energy of γ . See Figure 5.

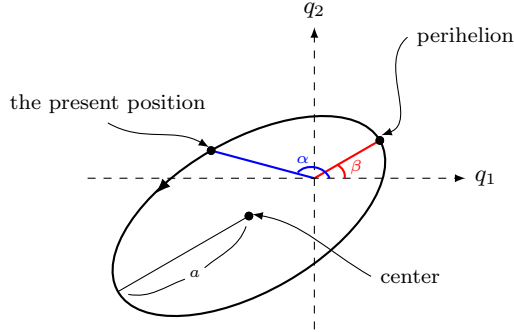


FIGURE 5. Some quantities associated with a Kepler ellipse of Kepler energy $E < 0$. The quantity a is the semi-major axis that is equal to $-\frac{1}{2E}$. The quantity α is given by the argument of the present position, and β is given by the argument of the perihelion.

Set $\mathcal{K} = \mathbb{R}/2\pi\mathbb{Z} \times \mathbb{R}/2\pi\mathbb{Z} \times S$, where $S = \{(x, y) \in \mathbb{R}^2 : x > 0, y \in (0, 1)\}$. Then there is a diffeomorphism

$$\mathcal{K}: \mathcal{E} \rightarrow \mathcal{K}, \quad (q_1, q_2, p_1, p_2) \mapsto (\alpha, \beta, a, e),$$

called the Kepler map. This implies that the domain \mathcal{E} is a thickened two-torus.

Theorem 4.1 (Lagrange, 1808). *The Kepler map \mathcal{K} satisfies*

$$\mathcal{K}_*(dp_1 \wedge dq_1 + dp_2 \wedge dq_2) = d\sqrt{a(1-e^2)} \wedge d\beta + d\sqrt{a} \wedge d(\alpha - \beta).$$

Suggested by this result, Delaunay (1860) considered a diffeomorphism

$$\mathcal{D}: \mathcal{K} \rightarrow \mathcal{D}, \quad (\alpha, \beta, a, e) \mapsto (\beta, \alpha - \beta, \sqrt{a(1 - e^2)}, \sqrt{a}),$$

where

$$\mathcal{D} := \mathbb{R}/2\pi\mathbb{Z} \times \mathbb{R}/2\pi\mathbb{Z} \times \mathcal{O}, \quad \mathcal{O} = \{(x, y) \in \mathbb{R}^2 : 0 < x < y\}.$$

Write

$$(l, k, L, K) = (\beta, \alpha - \beta, \sqrt{a(1 - e^2)}, \sqrt{a})$$

and define

$$\Delta = \mathcal{D} \circ \mathcal{K}: \mathcal{E} \rightarrow \mathcal{D}, \quad (q_1, q_2, p_1, p_2) \mapsto (l, k, L, K),$$

called the Delaunay map. Theorem 4.1 implies that Δ is a symplectomorphism, namely, it satisfies

$$\Delta_*(dp_1 \wedge dq_1 + dp_2 \wedge dq_2) = dL \wedge dl + dK \wedge dk.$$

However, since the argument of the perihelion is undefined for a circular orbit, the Delaunay map cannot be used to study the dynamics in a neighbourhood of a circular orbit.

Remark 4.2. The classical notations of the Delaunay variables are (g, l, G, L) , not (l, k, L, K) . However, we stick to our choice since we would like to denote the angular momentum by L .

To remedy this problem, Poincaré introduced new coordinates as follows. Define

$$\Pi: \mathcal{D} \rightarrow \mathbb{R} \times \mathbb{R}/2\pi\mathbb{Z} \times \mathbb{R} \times \mathbb{R}, \quad (l, k, L, K) \mapsto (\eta, \lambda, \xi, \Lambda),$$

where

$$\begin{aligned} \eta &= -\sqrt{2(K - L)} \sin l, \\ \lambda &= l + k, \\ \xi &= \sqrt{2(K - L)} \cos l, \\ \Lambda &= K. \end{aligned}$$

It turned out that Π is a symplectomorphism onto its image $\mathcal{P} = \Pi(\mathcal{D})$. We then define the Poincaré mapping

$$\mathcal{P} = \Pi \circ \Delta = \Pi \circ \mathcal{D} \circ \mathcal{K}: \mathcal{E} \rightarrow \mathcal{P},$$

which is a symplectomorphism as well. Namely, it satisfies

$$\mathcal{P}^*(d\xi \wedge d\eta + d\Lambda \wedge d\lambda) = dp_1 \wedge dq_1 + dp_2 \wedge dq_2.$$

We shall now add the circular orbits. Recall that for the circular orbits we have $e = 0, \alpha = \beta$ and $L = K$. Let

$$\begin{aligned} \bar{\mathcal{E}} &= \mathcal{E} \cup \{(q, p) \in T^*(\mathbb{R} \setminus \{0\}) : E(q, p) < 0 = e(q, p), L(q, p) > 0\} \\ &= \{(q, p) \in T^*(\mathbb{R} \setminus \{0\}) : E(q, p) < 0 \leq e(q, p) < 1, L(q, p) > 0\} \end{aligned}$$

and

$$\bar{\mathcal{P}} = \mathcal{P} \cup \{(0, \lambda, 0, \Lambda) : \lambda \in \mathbb{R}/2\pi\mathbb{Z}, \Lambda > 0\}.$$

If $e(q_1, q_2, p_1, p_2) = 0$, then we set

$$\mathcal{P}(q_1, q_2, p_1, p_2) = (0, \lambda, 0, \Lambda)$$

by defining $\lambda = \alpha$ and $\Lambda = L = K$. This extends the Poincaré mapping to a symplectomorphism $\mathcal{P}: \bar{\mathcal{E}} \rightarrow \bar{\mathcal{P}}$. We conclude that in the study of direct orbits, i.e. orbits with $L > 0$, we can work with the transformed Hamiltonian $\mathcal{P}_*H: \bar{\mathcal{P}} \rightarrow \mathbb{R}$.

We now consider

$$\bar{\mathcal{E}}' = \{(q, p) \in T^*(\mathbb{R}^2 \setminus \{0\}) : E(q, p) < 0 \leq e(q, p) < 1, L(q, p) < 0\}$$

and note that $\psi(\bar{\mathcal{E}}') = \bar{\mathcal{E}}$, where $\psi(q_1, q_2, p_1, p_2) = (q_1, q_2, -p_1, -p_2)$. Define $\phi: \bar{\mathcal{P}} \rightarrow \bar{\mathcal{P}}' := \phi(\bar{\mathcal{P}})$ by

$$\phi(\eta, \lambda, \xi, \Lambda) = (\eta, \lambda, -\xi, -\Lambda).$$

Then we obtain a symplectomorphism

$$\mathcal{P}' := \phi \circ \mathcal{P} \circ \psi: \bar{\mathcal{E}}' \rightarrow \bar{\mathcal{P}}'.$$

It follows that in the study of retrograde orbits, i.e. orbits with $L < 0$, we can work with the transformed Hamiltonian $\mathcal{P}'_* H: \bar{\mathcal{P}}' \rightarrow \mathbb{R}$.

5. BELOW THE CRITICAL ENERGY

Throughout the section we fix $c < -\frac{3}{2}$ and $E_0 \in (E_{\text{direct}}^u, 0)$. We shall prove the assertion of Theorem 1.1 for the set

$$\Sigma_{\text{direct}}^u = \{\text{all periodic orbits of } X_H \text{ with } E \in [E_{\text{direct}}^u, E_0]\} \subset \Sigma_c^u,$$

diffeomorphic to a solid torus with core being the direct circular orbit γ_{direct}^u . Note that it contains only direct orbits and no collision orbits. Indeed, every periodic orbit on Σ_{direct}^u has $L > 0$. See Lemma 3.1.

Remark 5.1. The neighbourhood Σ_{direct}^u of γ_{direct}^u could be arbitrarily large: just take $E_0 \in (E_{\text{direct}}^u, 0)$ to be sufficiently close to 0.

We shall work in Poincaré's coordinates. For simplicity we write $(x_1, x_2, y_1, y_2) = (\eta, \lambda, \xi, \Lambda)$. Note that

$$y_2 = \sqrt{a} = \frac{1}{\sqrt{-2E}}, \quad x_1^2 + y_1^2 = 2(y_2 - L).$$

Then the Hamiltonian (1.1) is given in Poincaré's coordinates by

$$H(x_1, x_2, y_1, y_2) = -\frac{1}{2y_2^2} - y_2 + \frac{1}{2}(x_1^2 + y_1^2) \quad (5.1)$$

for $(x_1, x_2, y_1, y_2) \in \bar{\mathcal{P}} \subset \mathbb{R} \times \mathbb{R}/2\pi\mathbb{Z} \times \mathbb{R} \times \mathbb{R}_+$. We set

$$H_1(x_1, y_1) = \frac{1}{2}(x_1^2 + y_1^2), \quad H_2(y_2) = -\frac{1}{2y_2^2} - y_2, \quad (5.2)$$

so that $H = H_1 + H_2$.

Since $E_0 \in (E_{\text{direct}}^u, 0)$ is fixed and we consider the subset $\Sigma_{\text{direct}}^u \subset \Sigma_c^u$, we have

$$y_2 \in [\Lambda_1, \Lambda_2] \quad \text{on } \Sigma_{\text{direct}}^u,$$

where $\Lambda_1 = \sqrt{-\frac{1}{2E_{\text{direct}}^u}}$ and $\Lambda_2 = \sqrt{-\frac{1}{2E_0}}$. Since $E_{\text{direct}}^u > -\frac{1}{2}$, see Lemma 3.1, we have $\Lambda_1 > 1$.

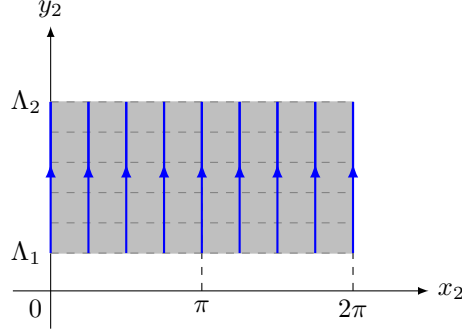


FIGURE 6. Negative gradient flow lines of H_2 . Dashed lines indicate Hamiltonian trajectories.

5.1. Disc foliation. It is easy to construct a disc foliation of Σ_{direct}^u transverse to the Hamiltonian flow by looking at the negative gradient flow lines of H_2 . These are solutions to the ODE

$$\dot{x}_2 = -(H_2)_{x_2} = 0, \quad \dot{y}_2 = -(H_2)_{y_2} = -\frac{1}{y_2^3} + 1 > 0.$$

Therefore, along every negative gradient flow line the x_2 -component is constant and the y_2 -component is strictly increasing. See Figure 6.

Pick any $x_2 \in \mathbb{R}/2\pi\mathbb{Z}$ and let h_{x_2} be the corresponding negative gradient flow line of H_2 . Denote by $\Pi: \Sigma_{\text{direct}}^u \rightarrow \mathbb{R}^2$ the projection $(x_1, x_2, y_1, y_2) \mapsto (x_2, y_2)$. Then the preimage $\Pi^{-1}(h_{x_2})$ is an embedded disc in Σ_{direct}^u that is transverse to the Hamiltonian flow. The point $\Pi^{-1}(x_2, \Lambda_1)$ is the intersection of the disc $\Pi^{-1}(h_{x_2})$ and the direct circular orbit γ_{direct}^u . By varying $x_2 \in \mathbb{R}/2\pi\mathbb{Z}$, we obtain the desired disc foliation.

Below we shall embed Σ_{direct}^u into a weakly convex three-sphere and construct a symmetric finite energy foliation of the three-sphere. We then obtain a disc foliation as the intersection of the projection of the finite energy foliation with Σ_{direct}^u .

5.2. Interpolation. Fix $\Lambda_3 \in (\Lambda_2, +\infty)$ and $0 < \varepsilon_0 < \frac{1}{2}(\Lambda_3 - \Lambda_2)$. Consider

$$F(x_2, y_2) = \frac{1}{2}(y_2 - \Lambda_3)^2 - \cos \frac{x_2}{2} + B,$$

where $(x_2, y_2) \in \mathbb{R}/4\pi\mathbb{Z} \times \mathbb{R}_+$, and the constant B satisfies

$$B < -\frac{1}{2(\Lambda_2 + \varepsilon_0)^2} - (\Lambda_2 + \varepsilon_0) - \frac{1}{2}(\Lambda_2 + \varepsilon_0 - \Lambda_3)^2 - 1 \quad (5.3)$$

and define

$$K(x_2, y_2) = (1 - f(y_2))H_2(y_2) + f(y_2)F(x_2, y_2), \quad (5.4)$$

where $f: \mathbb{R} \rightarrow [0, 1]$ is a non-decreasing function satisfying $f(y_2) = 0$ for $y_2 < \Lambda_2 + \varepsilon_0$ and $f(y_2) = 1$ for $y_2 > \Lambda_2 + 2\varepsilon_0$. See Figure 7.

Set

$$\bar{H}(x_1, x_2, y_1, y_2) = H_1(x_1, y_1) + K(x_2, y_2),$$

where $(x_2, y_2) \in \mathbb{R}/4\pi\mathbb{Z} \times \mathbb{R}_+$, and denote by $\bar{\Sigma}$ the connected component of $\bar{H}^{-1}(c)$ that contains a double cover $\bar{\Sigma}_{\text{direct}}^u$ of Σ_{direct}^u . Note that \bar{H} is invariant under the

anti-symplectic involution

$$\rho(x_1, x_2, y_1, y_2) = (-x_1, 4\pi - x_2, y_1, y_2). \quad (5.5)$$

We claim that for $y_2 \geq \Lambda_1$, the smooth function K has precisely two critical points $(0, \Lambda_3)$ that is a saddle and $(2\pi, \Lambda_3)$ that is a global minimum. In fact, we show that

$$K_{y_2} < 0, \quad \forall y_2 < \Lambda_3 \quad \text{and} \quad K_{y_2} > 0, \quad \forall y_2 > \Lambda_3. \quad (5.6)$$

It suffices to show that K is strictly decreasing in y_2 , provided $y_2 \in [\Lambda_2 + \varepsilon_0, \Lambda_2 + 2\varepsilon_0]$. We assume $y_2 \in [\Lambda_2 + \varepsilon_0, \Lambda_2 + 2\varepsilon_0]$ and find that

$$\begin{aligned} K_{y_2} = f' \cdot & \left(\frac{1}{2y_2^2} + y_2 + \frac{1}{2}(y_2 - \Lambda_3)^2 - \cos \frac{x_2}{2} + B \right) \\ & + (1 - f) \cdot \left(\frac{1}{y_2^3} - 1 \right) + f \cdot (y_2 - \Lambda_3). \end{aligned}$$

The first term in the right-hand side is non-positive due to the choice of the constant B . See (5.3). The second term is non-positive since $1 < \Lambda_2$, and the last term is also non-positive because of the choice of ε_0 . Note that at least one of the three terms is non-zero. This implies that K admits a critical point only if $y_2 = \Lambda_3$, provided $y_2 \geq \Lambda_1$. The rest of the claim is straightforward.

Given x_2 , define

$$\Lambda_{\max} = \Lambda_{\max}(x_2) := \max\{y_2 \mid (x_1, x_2, y_1, y_2) \in \bar{\Sigma}\}.$$

Notice that it satisfies $K(x_2, \Lambda_{\max}) = c$ and that

$$\Lambda_1 = \min\{y_2 \mid (x_1, x_2, y_1, y_2) \in \bar{\Sigma}\}.$$

We now introduce

$$G(x_2, y_2) = \frac{1}{2}x_2^2 + \frac{1}{2}(y_2 - \Lambda_3)^2.$$

Given $\varepsilon_1 > 0$, choose any non-decreasing smooth function $g: \mathbb{R} \rightarrow [0, 1]$ satisfying $g(x_2) = 0$ for $x_2 < -2\varepsilon_1$ and $g(x_2) = 1$ for $x_2 > -\varepsilon_1$ and define

$$\tilde{K}(x_2, y_2) = (1 - g(x_2))G(x_2, y_2) + g(x_2)K(x_2, y_2).$$

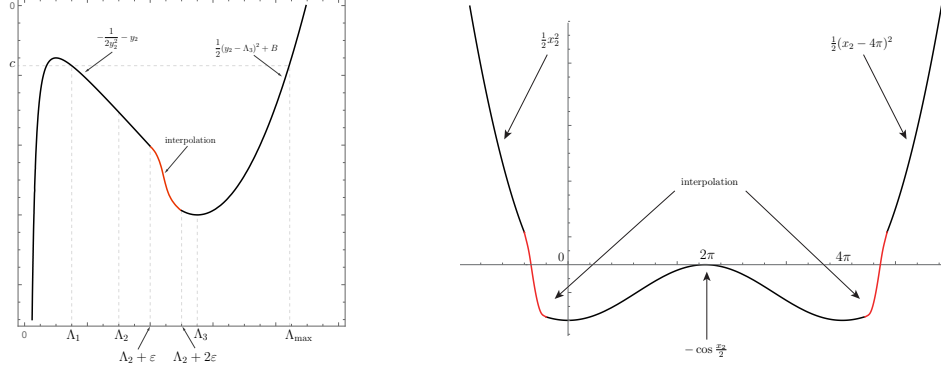
We repeat a similar business for $x_2 \geq 4\pi$ in a symmetric way (note that the function K is symmetric in x_2 with respect to $x_2 = 2\pi$). Namely, we interpolate between the smooth functions \tilde{K} and

$$\tilde{G}(x_2, y_2) = \frac{1}{2}(x_2 - 4\pi)^2 + \frac{1}{2}(y_2 - \Lambda_3)^2$$

using the non-increasing function $\tilde{g}(x_2) := g(4\pi - x_2)$. This produces a smooth function $\tilde{H}_2(x_2, y_2)$, which is still symmetric in x_2 with respect to $x_2 = 2\pi$. Note that we have broken the periodicity in x_2 . See Figure 7.

Lemma 5.2. *The function \tilde{H}_2 admits precisely three critical points $(x_2, y_2) = (0, \Lambda_3), (2\pi, \Lambda_3)$ and $(4\pi, \Lambda_3)$.*

Proof. By the definition and symmetry of \tilde{H}_2 , it suffices to show that there are no critical points of \tilde{H}_2 in $\{-2\varepsilon_1 < x_2 < -\varepsilon_1\}$.


 FIGURE 7. Interpolations for y_2 (left) and x_2 (right)

We assume $-2\varepsilon_1 < x_2 < -\varepsilon_1$ and find that

$$\begin{aligned} (\tilde{H}_2)_{x_2} &= (1 - g(x_2))x_2 + \frac{f(x_2)g(x_2)}{2} \sin \frac{x_2}{2} + g'(x_2)(K - G), \\ (\tilde{H}_2)_{y_2} &= (1 - g(x_2))(y_2 - \Lambda_3) + g(x_2)K_{y_2}. \end{aligned}$$

If $y_2 \geq \Lambda_1$, then we obtain in view of (5.6) that

$$(\tilde{H}_2)_{y_2} < 0, \quad \forall y_2 < \Lambda_3, \quad (\tilde{H}_2)_{y_2} > 0, \quad \forall y_2 > \Lambda_3,$$

and hence $(\tilde{H}_2)_{y_2}$ vanishes only if $y_2 = \Lambda_3$. We then compute

$$K(x_2, \Lambda_3) - G(x_2, \Lambda_3) = -\cos \frac{x_2}{2} - \frac{1}{2}x_2^2 + B < 0,$$

so that $(\tilde{H}_2)_{x_2}|_{y_2=\Lambda_3} < 0$.

Suppose that $y_2 < \Lambda_1$, so that

$$\begin{aligned} (\tilde{H}_2)_{x_2} &= (1 - g(x_2))x_2 + g'(x_2) \left(-\frac{1}{2y_2^2} - y_2 - \frac{1}{2}x_2^2 - \frac{1}{2}(y_2 - \Lambda_3)^2 \right), \\ (\tilde{H}_2)_{y_2} &= (1 - g(x_2))(y_2 - \Lambda_3) + g(x_2) \left(\frac{1}{y_2^3} - 1 \right). \end{aligned}$$

Note that $(\tilde{H}_2)_{y_2}$ may vanish for $y_2 < 1$. For $y_2 > 0$, a global minimum of the function $\frac{1}{2y_2^2} + y_2 + \frac{1}{2}(y_2 - \Lambda_3)^2$ is positive, and hence we have $(\tilde{H}_2)_{x_2} < 0$, provided $y_2 < 1$.

We conclude that there exist no critical points of \tilde{H}_2 in $\{-2\varepsilon_1 < x_2 < -\varepsilon_1\}$, from which the lemma follows. \square

We define the modified Hamiltonian

$$\tilde{H}(x_1, x_2, y_1, y_2) = H_1(x_1, y_2) + \tilde{H}_2(x_2, y_2).$$

The anti-symplectic involution ρ in (5.5) induces an anti-symplectic involution on $\mathbb{R}^3 \times \mathbb{R}_+$, again denoted by ρ . Note that \tilde{H} is ρ -invariant.

The previous lemma implies that the Hamiltonian \tilde{H} admits precisely three critical points

$$p_{c1} = (0, 0, 0, \Lambda_3), \quad p_{c2} = (0, 2\pi, 0, \Lambda_3), \quad p_{c3} = (0, 4\pi, 0, \Lambda_3). \quad (5.7)$$

Since $\tilde{H}(p_{c1}) = \tilde{H}(p_{c3}) = -1 + B < \tilde{H}(p_{c2}) = 1 + B < c$ and p_{c2} has Morse index 1 as a critical point of \tilde{H} , it follows from standard Morse theory that the energy level $\tilde{H}^{-1}(c)$ contains a unique connected component, denoted by Σ , which is diffeomorphic to S^3 . Note that Σ is ρ -invariant.

For later use, we prove the following assertion.

Lemma 5.3. *Along Σ we have $y_2 > 1$, and hence*

$$\tilde{H}_{y_2} < 0, \quad \forall y_2 < \Lambda_3, \quad \tilde{H}_{y_2} > 0, \quad \forall y_2 > \Lambda_3.$$

Proof. By the definition and symmetry of \tilde{H}_2 , without loss of generality we may assume that $-2\varepsilon_1 < x_2 < -\varepsilon_1$.

Fix $-2\varepsilon_1 < x_2 < -\varepsilon_1$ and consider the smooth function

$$Q(y_2) = \frac{1}{2}(1 - g(x_2))(y_2 - \Lambda_3)^2 + g(x_2) \left(-\frac{1}{2y_2^2} - y_2 \right), \quad y_2 > 0.$$

There is $a = a(x_2) \in (0, 1)$ such that the function Q is strictly increasing for $y_2 \in (0, a)$ and is strictly decreasing for $y_2 \in (a, \Lambda_2 + \varepsilon_0)$.

Every point $(x_1, x_2, y_1, y_2) \in \Sigma$ with $y_2 < \Lambda_2 + \varepsilon_0$ satisfies

$$Q(y_2) = c - \frac{1}{2}x_2^2(1 - g(x_2)) - \frac{1}{2}(x_1^2 + y_1^2),$$

and hence we find

$$\begin{aligned} Q(y_2) &\leq c - \frac{1}{2}x_2^2(1 - g(x_2)) \\ &< -\frac{3}{2}g(x_2) + \frac{1}{2}(1 - g(x_2))(1 - \Lambda_3)^2 \\ &= Q(1). \end{aligned}$$

This together with compactness of Σ implies that for any $(x_1, x_2, y_1, y_2) \in \Sigma$ with $x_2 \in (-2\varepsilon_1, -\varepsilon_1)$ the component y_2 is bigger than 1. The rest of the lemma is straightforward. This finishes the proof. \square

5.3. Construction of a contact form. In this section we construct a ρ -invariant Liouville vector field Y that is transverse to Σ . Then the restriction of the one-form $\omega_0(Y, \cdot)$ to Σ defines a contact form on Σ , denoted by λ . The anti-symplectic involution $\rho: \mathbb{R}^4 \rightarrow \mathbb{R}^4$ restricts to an anti-contact involution on Σ , still denoted by ρ . Consequently, we obtain a real contact manifold (Σ, λ, ρ) . Recall from Section 2.3 that ρ provides the exact anti-symplectic involution $\tilde{\rho} = \text{Id}_{\mathbb{R}} \times \rho$ on $(\mathbb{R} \times \Sigma, d(e^r \lambda))$.

We first claim that the radial vector field with respect to p_{c1}

$$Y_0 = \frac{1}{2}(x_1 \partial_{x_1} + x_2 \partial_{x_2} + y_1 \partial_{y_1} + (y_2 - \Lambda_3) \partial_{y_2})$$

is transverse to Σ along $\{x_2 < 2\pi\}$. By the definition of \tilde{H} , it suffices to consider the region $\{-2\varepsilon_1 < x_2 < 2\pi\}$. We find that

$$\begin{aligned} d\tilde{H}(Y_0) &= \frac{1}{2}(x_1^2 + y_1^2) + \frac{1}{2}(1 - g(x_2))(x_2^2 + (y_2 - \Lambda_3)^2) \\ &\quad + \frac{1}{2}g(x_2)(x_2 K_{x_2} + (y_2 - \Lambda_3) K_{y_2}) + \frac{1}{2}x_2 g'(x_2)(K - G). \end{aligned}$$

The first two terms in the right-hand side are non-negative. The third term is also non-negative because of Lemma 5.3 and (5.6). For the last term, we find that

$$\begin{aligned} & K(x_2, y_2) - G(x_2, y_2) \\ &= (1 - f(y_2)) \left(-\frac{1}{2y_2^2} - y_2 - \frac{1}{2}(y_2 - \Lambda_3)^2 \right) + f(y_2) \left(B - \cos \frac{x_2}{2} \right) - \frac{1}{2}x_2^2. \end{aligned}$$

By the choice of the constant B (see (5.3)), it is negative. This proves the claim.

We now consider the Liouville vector field

$$Y_1 = \frac{1}{2}(x_1\partial_{x_1} + y_1\partial_{y_1}) + \frac{1}{4}\sin \frac{x_2}{2}\partial_{x_2} + (y_2 - \Lambda_3) \left(1 - \frac{1}{8}\cos \frac{x_2}{2} \right) \partial_{y_2}.$$

Using (5.6) it is straightforward to see that $d\tilde{H}(Y_1) > 0$ along $\Sigma \cap \{0 < x_2 < 4\pi\}$.

In order to interpolate between the two Liouville vector fields Y_0 and Y_1 , we define a smooth function

$$\ell(x_2, y_2) = (y_2 - \Lambda_3) \left(\frac{1}{4}\sin \frac{x_2}{2} - \frac{1}{2}x_2 \right),$$

so that $X_\ell = Y_1 - Y_0$. Fix $\varepsilon_2 > 0$ small enough and pick any non-decreasing smooth function $h: \mathbb{R} \rightarrow [0, 1]$ satisfying $h(x_2) = 0$ for $x_2 < 2\pi - 2\varepsilon_2$ and $h(x_2) = 1$ for $x_2 > 2\pi - \varepsilon_2$. Define

$$\tilde{Y} = Y_0 + X_{h\ell}, \quad (5.8)$$

where $X_{h\ell}$ indicates the Hamiltonian vector field associated with $h(x_2)\ell(x_2, y_2)$.

We claim that the Liouville vector field \tilde{Y} is transverse to Σ along $\{x_2 < 4\pi\}$. In view of the argument above, it suffices to consider the region $\{2\pi - 2\varepsilon_2 < x_2 < 2\pi - \varepsilon_2\}$. We find that

$$d\tilde{H}(\tilde{Y}) = (1 - h)d\tilde{H}(Y_0) + hd\tilde{H}(Y_1) + \ell d\tilde{H}(X_h).$$

The sum of the first two terms in the right-hand side above is positive. For the last term, we find

$$\ell d\tilde{H}(X_h) = -h'(x_2) \cdot \left(\frac{1}{4}\sin \frac{x_2}{2} - \frac{1}{2}x_2 \right) (y_2 - \Lambda_3) K_{y_2}.$$

This is non-negative because of (5.6). This proves the claim.

We now repeat the same business as above in the region $\{x_2 > 2\pi\}$. More precisely, we consider the radial vector field with respect to p_{c2}

$$Y_2 = \frac{1}{2}(x_1\partial_{x_1} + (x_2 - 4\pi)\partial_{x_2} + y_1\partial_{y_1} + (y_2 - \Lambda_3)\partial_{y_2})$$

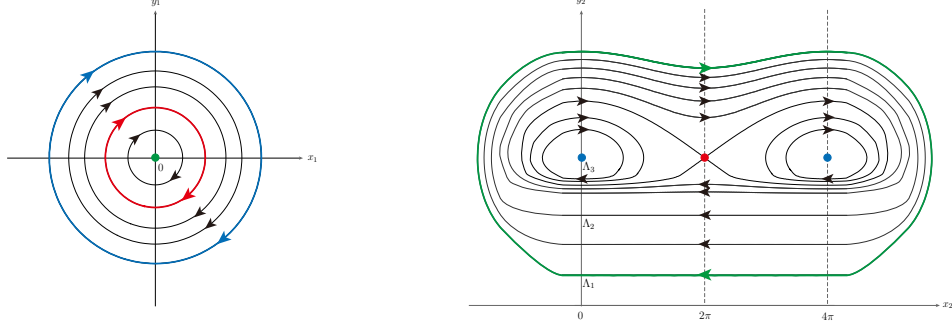
and interpolate between \tilde{Y} and Y_2 using the non-increasing function $\tilde{h}(x_2) := h(4\pi - x_2)$. This provides the Liouville vector field Y that is transverse to Σ . By construction, it is invariant under ρ .

5.4. Periodic orbits. Let $\gamma(t) = (x_1(t), x_2(t), y_1(t), y_2(t))$ be a periodic orbit of \tilde{H} . Denote by

$$\gamma_1(t) = (x_1(t), y_1(t)), \quad \gamma_2(t) = (x_2(t), y_2(t))$$

the projections of $\gamma(t)$ to the (x_1, y_1) -plane and to the (x_2, y_2) -plane, respectively. Then the periodic orbit γ belongs to one of the following three categories:

- γ_1 is constant; the green curve in Figure 8.
- γ_2 is constant; the red and blue curves in Figure 8.
- Both γ_1 and γ_2 are non-constant; the black curves in Figure 8.

FIGURE 8. Phase portraits of K_1 (left) and K_2 (right)

Consider the first case, so that we have $\gamma_1 \equiv (0, 0)$, and hence $\tilde{H}_2(\gamma_2(t)) = c, \forall t$. The corresponding periodic orbit will be denoted by P_0 .

We now assume that γ_2 is constant, so that we have either $\gamma_2 \equiv (0, \Lambda_3)$, $\gamma_2 \equiv (2\pi, \Lambda_3)$ or $\gamma_2 \equiv (4\pi, \Lambda_3)$. See Lemma 5.2. The corresponding periodic orbits γ will be denoted by $P_3 = (w_3, 2\pi)$, $P_2 = (w_2, 2\pi)$ and $P'_3 = (w'_3, 2\pi)$, where

$$\begin{aligned} w_3(t) &= (r_3 \sin t, 0, r_3 \cos t, \Lambda_3), \\ w_2(t) &= (r_2 \sin t, 2\pi, r_2 \cos t, \Lambda_3), \\ w'_3(t) &= (r_3 \sin t, 4\pi, r_3 \cos t, \Lambda_3), \end{aligned}$$

respectively, with

$$r_2 = \sqrt{2(c-1-B)} < r_3 = \sqrt{2(c+1-B)}. \quad (5.9)$$

Note that P_2 is a symmetric periodic orbit and that $P'_3 = (P_3)_\rho$. Since

$$R = \frac{1}{\lambda(X_{\tilde{H}})} X_{\tilde{H}},$$

the Reeb periods of P_2, P_3 and P'_3 are given by

$$\tau_2 = \pi r_2^2, \quad \tau_3 = \tau'_3 = \pi r_3^2,$$

respectively.

In the last case, i.e. both γ_1 and γ_2 are non-constant, the periodic orbit γ lies in an S^1 -family of periodic orbits.

5.5. Conley-Zehnder indices. We shall prove

Proposition 5.4. *The contact form λ on Σ , constructed in Section 5.3, is weakly convex. More precisely, the periodic orbits P_2, P_3 and P'_3 are non-degenerate and satisfy $\mu_{\text{CZ}}(P_2) = 2$ and $\mu_{\text{CZ}}(P_3) = \mu_{\text{CZ}}(P'_3) = 3$. The other periodic orbits have the Conley-Zehnder indices at least 3. In particular, P_2 is a unique periodic orbit having $\mu_{\text{CZ}} = 2$.*

Proof. We follow [26].

We first consider the periodic orbits P_2, P_3 and P'_3 . Since $\mu_{\text{CZ}}(P'_3) = \mu_{\text{CZ}}(P_3)$, see Section 2.2, we may consider only P_2 and P_3 along which we have

$$X_1 = (0, -r_i \cos t, 0, -r_i \sin t), \quad X_2 = (0, -r_i \sin t, 0, r_i \cos t), \quad i = 2, 3$$

where X_1 and X_2 are as in (2.1). As before, we denote by \mathfrak{T} the trivialisation of $(T\Sigma/\mathbb{R}X_K)|_{P_i}$ induced by X_1 and X_2 . We choose another trivialisation Φ that is induced by the canonical basis

$$V_1 = (0, 1, 0, 0), \quad V_2 = (0, 0, 0, 1).$$

In this trivialisation the linearised Hamiltonian flow along P_i restricted to $(T\Sigma/\mathbb{R}X_K)|_{P_i}$ is described by a solution to the ODE

$$\dot{\alpha}_i(s) = A\alpha_i(s), \quad A = \begin{pmatrix} 0 & 1 \\ -\frac{1}{4}\cos\frac{x_2}{2} & 0 \end{pmatrix}.$$

If $i = 2$, then we have $x_2 = 2\pi$, and hence

$$A \begin{pmatrix} 1 \\ 0 \end{pmatrix} = \begin{pmatrix} 0 \\ \frac{1}{4} \end{pmatrix}, \quad A \begin{pmatrix} 0 \\ 1 \end{pmatrix} = \begin{pmatrix} 1 \\ 0 \end{pmatrix}.$$

This implies that the rotation interval (see (2.4)) of any non-trivial solution to the ODE above contains 0 as an interior point. Since the winding number of the projection of X_1 (and hence also of X_2) to the (x_2, y_2) -plane are equal to 1, it follows that the rotation interval of any non-trivial solution to ODE (2.3) contains 2π as an interior point. We conclude from the definition of the Conley-Zehnder index that P_2 is non-degenerate and satisfies

$$\mu_{\text{CZ}}(P_2) = 2.$$

Consider P_3 , so that $x_2 = 0$. Then a continuous argument of any non-vanishing solution α to the ODE above is of the form

$$\vartheta(s) = -\frac{1}{2}s + \vartheta_0$$

for some constant $\vartheta_0 \in \mathbb{R}$. Since the Hamiltonian period of P_3 equals 2π , the rotation interval of α is contained in $(-2\pi, 0)$. Since the basis $\{X_1, X_2\}$ has the negative orientation with respect to the basis $\{V_1, V_2\}$, and the winding number of the projection of X_1 to the (x_2, y_2) -plane equals 1, as in the previous case, this implies that the rotation interval of any non-trivial solution to ODE (2.3) is contained in $(2\pi, 4\pi)$ from which we obtain that P_3 is non-degenerate and satisfies

$$\mu_{\text{CZ}}(P_3) = 3.$$

Let $P = (w, T)$ be a periodic orbit not corresponding to the critical points of \tilde{H}_2 . See Figure 8. We write $w(t) = (x_1(t), x_2(t), y_1(t), y_2(t))$ and denote by $w_1(t) = (x_1(t), y_1(t))$ and $w_2(t) = (x_2(t), y_2(t))$ the projections of $w(t)$ to the (x_1, y_1) -plane and (x_2, y_2) -plane, respectively. Note that

$$\dot{w}_2(t) = (\dot{x}_2(t), \dot{y}_2(t)) = \left(\tilde{H}_{y_2}(w(t)), -\tilde{H}_{x_2}(w(t)) \right).$$

For $j = 1, 2$, $w_j(t)$ is a closed curve which is oriented in the clockwise direction, and hence its winding number with respect to the standard basis is given by

$$\text{wind}(t \mapsto \dot{w}_j(t)) \leq -1,$$

where the equality holds if and only if $w_j(t)$ is a simple closed curve.

We abbreviate by

$$Y_1(t) = \left(\tilde{H}_{y_2}(w(t)), \tilde{H}_{x_2}(w(t)) \right), \quad Y_2(t) = \left(\tilde{H}_{x_2}(w(t)), -\tilde{H}_{y_2}(w(t)) \right),$$

which are the projections of X_1 and X_2 along P to the (x_1, y_1) -plane. Since P does not correspond to the critical points of \tilde{H}_2 , these vectors are non-vanishing

and linearly independent. Hence, we may compute the rotation interval associated with the transverse linearised flow of X_K along P using the trivialisation of the (x_1, y_1) -plane induced by Y_1 and Y_2 . We find the winding numbers of Y_1 and Y_2 with respect to the standard basis

$$\begin{aligned}
\text{wind}(t \mapsto Y_1(t)) &= \text{wind}(t \mapsto Y_2(t)) \\
&= \text{wind}\left(t \mapsto (\tilde{H}_{y_2}(w(t)), \tilde{H}_{x_2}(w(t)))\right) \\
&= -\text{wind}\left(t \mapsto (\tilde{H}_{y_2}(w(t)), -\tilde{H}_{x_2}(w(t)))\right) \quad (5.10) \\
&= -\text{wind}(t \mapsto \dot{w}_2(t)) \\
&\geq 1.
\end{aligned}$$

Suppose that P corresponds to a black curve in Figure 8, so that $\dot{w}_1(t)$ is non-vanishing. Since $\dot{w}_1(t)$ is preserved by the linearised flow projected to the (x_1, y_1) -plane, there is a solution $\alpha(t)$ to ODE (2.3) whose projection to the (x_1, y_1) -plane equals $\dot{w}_1(t)$. We denote such a projection by $\bar{\alpha}(t)$ and then compute its winding number with respect to the basis $\mathfrak{B} = \{Y_1(t), Y_2(t)\}$

$$\begin{aligned}
\text{wind}(t \mapsto \bar{\alpha}(t); \mathfrak{B}) &= \text{wind}(t \mapsto Y_1(t)) - \text{wind}(t \mapsto \bar{\alpha}(t)) \\
&= \text{wind}(t \mapsto Y_1(t)) - \text{wind}(t \mapsto \dot{w}_1(t)) \\
&\geq 2,
\end{aligned}$$

where we have used the fact that the basis \mathfrak{B} has negative orientation with respect to the standard basis. This implies that the rotation interval of P contains 4π , from which we conclude that $\mu_{CZ}(P) \geq 3$.

We now assume that P corresponds to the green curve in Figure 8, so that $w_1(t) \equiv (0, 0)$. In this case, the linearised Hamiltonian flow along P restricted to the (x_1, y_1) -plane is described by a solution to the ODE

$$\dot{\beta} = \begin{pmatrix} 0 & 1 \\ -1 & 0 \end{pmatrix} \beta.$$

As in the case of P_3 , this implies that the rotation interval of β is contained in $(-\infty, 0)$, and hence we find using (5.10) that the rotation interval of any non-trivial solution to ODE (2.3) is contained in $(2\pi, +\infty)$. Consequently, we have $\mu_{CZ}(P) \geq 3$.

This finishes the proof. \square

5.6. Construction of a finite energy foliation. Let \bar{X}_1, \bar{X}_2 be the two vector fields that span the contact structure $\xi = \ker \lambda$, see (2.2). We define the $d\lambda$ -compatible almost complex structure $J: \xi \rightarrow \xi$ by

$$J(\bar{X}_1) = \bar{X}_2. \quad (5.11)$$

Note that it is ρ -anti-invariant. See (2.6).

Abbreviate $S^1 = \mathbb{R}/\mathbb{Z}$. Let $\tilde{u} = (a, u): \mathbb{R} \times S^1 \rightarrow \mathbb{R} \times \Sigma$ be a \tilde{J} -holomorphic curve, where \tilde{J} is given as in (2.5). Being \tilde{J} -holomorphic, \tilde{u} satisfies

$$\begin{cases} \pi u_s + J(u)\pi u_t = 0, \\ \lambda(u_t) = a_s, \\ \lambda(u_s) = -a_t, \end{cases} \quad (5.12)$$

where $\pi: T\Sigma \rightarrow \xi$ is the projection along R . We make the following Ansatz:

Ansatz. The Σ -part u of \tilde{u} takes the form

$$u(s, t) = (r(s) \sin 2\pi t, x_2(s), r(s) \cos 2\pi t, y_2(s)) \quad (5.13)$$

with $r(s) \neq 0$ and $\dot{r}(s) \neq 0$.

We only consider the case that we have $x_2 \equiv 0, x_2 \equiv 2\pi, x_2 \equiv 4\pi$ or $y_2 \equiv \Lambda_3$ with $0 \leq x_2(s) \leq 4\pi, \forall s$. Recall that in this case we have $\tilde{H}_2 = K$, where the latter is as in (5.4). Since $u(s, t) \in \Sigma$, this implies that

$$\frac{1}{2}r(s)^2 + K(x_2(s), y_2(s)) = c. \quad (5.14)$$

Following the argument given in [6, Chapter 5] we shall show that the corresponding \tilde{u} is a finite energy plane asymptotic to P_2, P_3 or P'_3 or a finite energy cylinder asymptotic to P_3 or P'_3 at its positive puncture and to P_2 at its negative puncture.

We first assume the case where $x_2(s) \in [0, 2\pi], \forall s$, so that the Liouville vector field is given by $Y = Y_0 + X_{h\ell}$, see (5.8), and hence the contact form λ equals

$$\begin{aligned} \lambda &= \frac{1}{2}(y_1 dx_1 + (y_2 - \Lambda_3) dx_2 - x_1 dy_1 - x_2 dy_2) - d(h\ell) \\ &= \frac{1}{2}y_1 dx_1 - \frac{1}{2}x_1 dy_1 - \frac{1}{2}(x_2 + h(x_2))\left(\frac{1}{2}\sin\frac{x_2}{2} - x_2\right) dy_2 \\ &\quad + \frac{1}{2}(y_2 - \Lambda_3)\left(1 - h'(x_2)\left(\frac{1}{2}\sin\frac{x_2}{2} - x_2\right) - h(x_2)\left(\frac{1}{4}\cos\frac{x_2}{2} - 1\right)\right) dx_2. \end{aligned}$$

We compute

$$\begin{aligned} \lambda(u_t) &= \pi r^2, \\ \lambda(u_s) &= -\frac{1}{2}(x_2 + h(x_2))\left(\frac{1}{2}\sin\frac{x_2}{2} - x_2\right)\dot{y}_2 \\ &\quad + \frac{1}{2}(y_2 - \Lambda_3)\left(1 - h'(x_2)\left(\frac{1}{2}\sin\frac{x_2}{2} - x_2\right) - h(x_2)\left(\frac{1}{4}\cos\frac{x_2}{2} - 1\right)\right)\dot{x}_2. \end{aligned}$$

Since $x_2 \equiv 0, x_2 \equiv 2\pi$ or $y_2 \equiv \Lambda_3$, we obtain

$$\lambda(u_s) = 0.$$

This together with the last identity of (5.12) implies that a is independent of t , so we may choose

$$a(s, t) = a(s) = \int_0^s \pi r(u)^2 du \quad (5.15)$$

from which we see that $a \rightarrow \pm\infty$ as $s \rightarrow \pm\infty$.

The first identity of (5.12) implies that πu_s and πu_t are linearly independent, so that there exist A, B, C and D such that

$$\bar{X}_1 = A\pi u_s + B\pi u_t \quad \text{and} \quad \bar{X}_2 = C\pi u_s + D\pi u_t.$$

By definition of J , we have $A = D$ and $B = -C$, and hence

$$\bar{X}_1 = A\pi u_s + B\pi u_t \quad \text{and} \quad \bar{X}_2 = -B\pi u_s + A\pi u_t. \quad (5.16)$$

Let $P: \mathbb{R}^4 \rightarrow \mathbb{R}^2$ be the projection $(x_1, x_2, y_1, y_2) \mapsto (x_2, y_2)$ and denote

$$P(\bar{X}_1) = \begin{pmatrix} \square_1 \\ \square_2 \end{pmatrix}, \quad P(\bar{X}_2) = \begin{pmatrix} \triangle_1 \\ \triangle_2 \end{pmatrix}, \quad P(\pi u_s) = \begin{pmatrix} a_1 \\ a_2 \end{pmatrix}, \quad P(\pi u_t) = \begin{pmatrix} b_1 \\ b_2 \end{pmatrix}.$$

A direct computation using (5.14) shows that

$$a_1 b_2 - a_2 b_1 = -\frac{\pi r^3 \dot{r}}{k} \neq 0,$$

where

$$\begin{aligned} k &= \lambda(X_{\tilde{H}}) \\ &= \frac{r^2}{2} + \frac{1}{2}(y_2 - \Lambda_3)(1 - h'(x_2)(\frac{1}{2} \sin \frac{x_2}{2} - x_2) - h(x_2)(\frac{1}{4} \cos \frac{x_2}{2} - 1))K_{y_2} \\ &\quad + \frac{1}{2}(x_2 + h(x_2)(\frac{1}{2} \sin \frac{x_2}{2} - x_2))K_{x_2}. \end{aligned}$$

By means of (5.16) we obtain

$$\frac{1}{a_1 b_2 - a_2 b_1} \begin{pmatrix} b_2 & -b_1 \\ -a_2 & a_1 \end{pmatrix} \begin{pmatrix} \square_1 \\ \square_2 \end{pmatrix} = \begin{pmatrix} A \\ B \end{pmatrix} = \frac{1}{a_1 b_2 - a_2 b_1} \begin{pmatrix} -a_2 & a_1 \\ -b_2 & b_1 \end{pmatrix} \begin{pmatrix} \triangle_1 \\ \triangle_2 \end{pmatrix},$$

and hence

$$\begin{aligned} b_2 \square_1 - b_1 \square_2 &= -a_2 \triangle_1 + a_1 \triangle_2, \\ -a_2 \square_1 + a_1 \square_2 &= -b_2 \triangle_1 + b_1 \triangle_2. \end{aligned} \tag{5.17}$$

We compute that

$$\triangle_1 \square_2 - \triangle_2 \square_1 = \frac{r^2(r^2 + K_{x_2}^2 + K_{y_2}^2)}{2k} > 0.$$

Then solving (5.17) provides

$$\begin{aligned} \begin{pmatrix} \dot{x}_2 \\ \dot{y}_2 \end{pmatrix} &= \frac{1}{\triangle_1 \square_2 - \triangle_2 \square_1} \begin{pmatrix} -\square_1 & \triangle_1 \\ -\square_2 & \triangle_2 \end{pmatrix} \begin{pmatrix} b_2 \square_1 - b_1 \square_2 \\ -b_2 \triangle_1 + b_1 \triangle_2 \end{pmatrix} \\ &= \frac{1}{\triangle_1 \square_2 - \triangle_2 \square_1} \begin{pmatrix} -b_2(\triangle_1^2 + \square_1^2) + b_1(\triangle_1 \triangle_2 + \square_1 \square_2) \\ b_1(\triangle_2^2 + \square_2^2) - b_2(\triangle_1 \triangle_2 + \square_1 \square_2) \end{pmatrix}. \end{aligned} \tag{5.18}$$

Suppose first that $x_2 \equiv 0$. Using (5.14) and (5.18) we find

$$\dot{y}_2(s) = \frac{-2\pi r(s)^2 K_{y_2}(0, y_2(s))}{(K_{y_2}(0, y_2(s)))^2 + r(s)^2} = \frac{-4\pi(c - K(0, y_2(s)))K_{y_2}(0, y_2(s))}{(K_{y_2}(0, y_2(s)))^2 + 2(c - K(0, y_2(s)))}, \tag{5.19}$$

which may be seen as a differential equation of the type

$$\dot{y}_2(s) = P(y_2(s)). \tag{5.20}$$

Here, $P = P(y_2)$ is a smooth function defined on the interval $[y_2^-, y_2^+]$, where $(y_2^-, y_2^+) = (\Lambda_1, \Lambda_3)$ or $(y_2^-, y_2^+) = (\Lambda_3, \Lambda_{\max})$. It follows from (5.6) that the function P satisfies the following properties:

$$\begin{cases} P(y_2) = 0 & y_2 = \Lambda_1, \Lambda_3, \Lambda_{\max}, \\ P(y_2) > 0 & y_2 \in (\Lambda_1, \Lambda_3), \\ P(y_2) < 0 & y_2 \in (\Lambda_3, \Lambda_{\max}). \end{cases} \tag{5.21}$$

Thus, any solution $y_2 = y_2(s)$ to ODE (5.19) with initial condition $y_2(0) \in (\Lambda_1, \Lambda_3)$ is strictly increasing and satisfies

$$\lim_{s \rightarrow -\infty} y_2(s) = \Lambda_1 \quad \text{and} \quad \lim_{s \rightarrow +\infty} y_2(s) = \Lambda_3,$$

and any solution with $y_2(0) \in (\Lambda_3, \Lambda_{\max})$ is strictly decreasing and satisfies

$$\lim_{s \rightarrow -\infty} y_2(s) = \Lambda_{\max} \quad \text{and} \quad \lim_{s \rightarrow +\infty} y_2(s) = \Lambda_3.$$

By construction such a solution yields a solution

$$u(s, t) = (r(s) \sin 2\pi t, 0, r(s) \cos 2\pi t, y_2(s)), \quad (s, t) \in \mathbb{R} \times S^1 \quad (5.22)$$

to the first equation in (5.12). Here, the radius $r(s)$ is determined by relation (5.14) with $x_2(s) = 0$ and satisfies

$$\lim_{s \rightarrow -\infty} r(s) = 0, \quad \lim_{s \rightarrow +\infty} r(s) = r_3,$$

where r_3 is as in (5.9). This together with $a(s, t)$, defined in (5.15), produces a \tilde{J} -holomorphic curve $\tilde{u} = (a, u): \mathbb{R} \times S^1 \rightarrow \mathbb{R} \times \Sigma$. Note that this solution depends on the choice of the initial condition $y_2(0) \in (\Lambda_1, \Lambda_3) \cup (\Lambda_3, \Lambda_{\max})$. For any $N > 0$ and for any $\phi: \mathbb{R} \rightarrow [0, 1]$ with $\phi' \geq 0$, we have

$$\int_{[-N, N] \times S^1} d\tilde{u}^*(\phi\lambda) = \phi(a(N))\pi r(N)^2 - \phi(a(-N))\pi r(-N)^2,$$

and hence

$$E(\tilde{u}) = \tau_3 = \pi r_3^2.$$

Moreover, the mass of \tilde{u} at $-\infty$ is given by

$$m(-\infty) = \lim_{N \rightarrow -\infty} \int_{\{N\} \times S^1} u^*\lambda = \lim_{N \rightarrow -\infty} \pi r(N)^2 = 0,$$

implying that $-\infty$ is a removable puncture of \tilde{u} . See [10, Section 1]. After removing it, we obtain an embedded finite energy \tilde{J} -holomorphic plane $\tilde{u} = (a, u): \mathbb{C} \rightarrow \mathbb{R} \times \Sigma$ asymptotic to P_3 at its positive puncture $s = +\infty$.

In the case $x_2 \equiv 2\pi$, we obtain

$$\dot{y}_2(s) = \frac{-4\pi(c - K(2\pi, y_2(s)))K_{y_2}(2\pi, y_2(s))}{(K_{y_2}(2\pi, y_2(s)))^2 + 2(c - K(2\pi, y_2(s)))}, \quad (5.23)$$

which may be seen as a differential equation satisfying the same properties as above. See (5.20) and (5.21). Note that the radius $r(s)$, determined by (5.14) with $x_2(s) = 2\pi$, satisfies

$$\lim_{s \rightarrow -\infty} r(s) = 0, \quad \lim_{s \rightarrow +\infty} r(s) = r_2,$$

where r_2 is as in (5.9). Then arguing in a similar manner we find an embedded finite energy \tilde{J} -holomorphic plane \tilde{u} , depending on the initial condition $y_2(0) \in (\Lambda_1, \Lambda_3) \cup (\Lambda_3, \Lambda_{\max})$, asymptotic to P_2 at its positive puncture $s = +\infty$ and having energy equal to $\tau_2 = \pi r_2^2$. Note that it is invariant, i.e. $\tilde{u} = \tilde{u}_\rho$. See Section 2.3.

Finally, assume that $y_2 \equiv \Lambda_3$ with $0 \leq x_2(s) \leq 2\pi, \forall s$, so that

$$\dot{x}_2(s) = \frac{-4\pi(c - K(x_2(s), \Lambda_3))K_{x_2}(x_2(s), \Lambda_3)}{(K_{x_2}(x_2(s), \Lambda_3))^2 + 2(c - K(x_2(s), \Lambda_3))}, \quad (5.24)$$

which may be seen as a differential equation of the type

$$\dot{x}_2(s) = Q(x_2(s)).$$

Here, $Q = Q(x_2)$ is a smooth function defined on $[0, 2\pi]$. Notice that

$$\begin{cases} Q(x_2) = 0 & x_2 = 0, 2\pi, \\ Q(x_2) < 0 & 0 < x_2 < 2\pi, \end{cases}$$

from which we see that any solution $x_2 = x_2(s)$ to ODE (5.24) with initial condition $x_2(0) \in (0, 2\pi)$ is strictly decreasing and satisfies

$$\lim_{s \rightarrow -\infty} x_2(s) = 2\pi \quad \text{and} \quad \lim_{s \rightarrow +\infty} x_2(s) = 0.$$

In view of the construction such a solution gives rise to a solution

$$u(s, t) = (r(s) \sin 2\pi t, x_2(s), r(s) \cos 2\pi t, \Lambda_3), \quad (s, t) \in \mathbb{R} \times S^1 \quad (5.25)$$

to the first equation in (5.12). The radius $r(s)$ is determined by (5.14) with $y_2(s) = \Lambda_3$ and satisfies

$$\lim_{s \rightarrow -\infty} r(s) = r_2 \quad \text{and} \quad \lim_{s \rightarrow +\infty} r(s) = r_3,$$

where r_2 and r_3 are as in (5.9). This together with $a(s, t)$, defined in (5.15), produces a \tilde{J} -holomorphic curve $\tilde{u} = (a, u): \mathbb{R} \times S^1 \rightarrow \mathbb{R} \times \Sigma$, depending on the choice of the initial condition $x_2(0) \in (0, 2\pi)$. The Hofer energy is given by τ_3 and the mass of \tilde{u} at $-\infty$ is equal to $\tau_2 = \pi r_2^2$, implying that $-\infty$ is non-removable. Thus, we obtain an embedded finite energy \tilde{J} -holomorphic cylinder $\tilde{v} = (b, v): \mathbb{R} \times S^1 \rightarrow \mathbb{R} \times \Sigma$ asymptotic to P_3 at its positive puncture $s = +\infty$ and to P_2 at its negative puncture $s = -\infty$.

We now consider the case $x_2 \equiv 4\pi$ or $y_2 \equiv \Lambda_3$ with $2\pi \leq x_2(s) \leq 4\pi, \forall s$. Instead of the direct construction as above, we shall use the symmetry induced by the anti-contact involution ρ .

Let $\tilde{u} = (a, u): \mathbb{C} \rightarrow \mathbb{R} \times \Sigma$, where $u(s, t)$ is as in (5.22), be a finite energy \tilde{J} -holomorphic plane, corresponding to $x_2 \equiv 0$. It is asymptotic to P_3 at its positive puncture. The discussion above shows that $\tilde{u}_\rho(s, t) = (a_\rho(s, t), u_\rho(s, t))$, where

$$a_\rho(s, t) = a(s, -t) \quad \text{and} \quad u_\rho(s, t) = (r(s) \sin 2\pi t, 4\pi, r(s) \cos 2\pi t, y_2(s)),$$

is a finite energy \tilde{J} -holomorphic plane asymptotic to $P'_3 = (P_3)_\rho$. As above, if $y_2(0) \in (\Lambda_1, \Lambda_3)$, then $y_2(s)$ is strictly increasing and satisfies

$$\lim_{s \rightarrow -\infty} y_2(s) = \Lambda_1 \quad \text{and} \quad \lim_{s \rightarrow +\infty} y_2(s) = \Lambda_3,$$

and if $y_2(0) \in (\Lambda_3, \Lambda_{\max})$, then $y_2(s)$ is strictly decreasing and satisfies

$$\lim_{s \rightarrow -\infty} y_2(s) = \Lambda_{\max} \quad \text{and} \quad \lim_{s \rightarrow +\infty} y_2(s) = \Lambda_3.$$

In a similar manner, if $\tilde{u} = (a, u): \mathbb{R} \times S^1 \rightarrow \mathbb{R} \times \Sigma$, where $u(s, t)$ is as in (5.25) and $0 \leq x_2(s) \leq 2\pi, \forall s$, is a finite energy \tilde{J} -holomorphic cylinder, then $\tilde{u}_\rho(s, t) = (a_\rho(s, t), u_\rho(s, t))$, where a_ρ is as above and

$$u_\rho(s, t) = (r(s) \sin 2\pi t, 4\pi - x_2(s), r(s) \cos 2\pi t, \Lambda_3),$$

is a finite energy \tilde{J} -holomorphic cylinder, asymptotic to $P'_3 = (P_3)_\rho$ at its positive puncture and to $P_2 = (P_2)_\rho$ at its negative puncture. Moreover, if $4\pi - x_2(s)$ has the initial condition $4\pi - x_2(0) \in (2\pi, 4\pi)$, then it is strictly increasing and satisfies

$$\lim_{s \rightarrow -\infty} 4\pi - x_2(s) = 2\pi \quad \text{and} \quad \lim_{s \rightarrow +\infty} 4\pi - x_2(s) = 4\pi.$$

We have constructed the following embedded finite energy \tilde{J} -holomorphic curves:

- finite energy planes $\tilde{u}_{3,1}$ and $\tilde{u}_{3,2}$, which corresponds to $x_2 \equiv 0$ and initial conditions $y_2(0) \in (\Lambda_1, \Lambda_3)$ and $y_2(0) \in (\Lambda_3, \Lambda_{\max})$, respectively. They are both asymptotic to P_3 .
- finite energy planes $\tilde{u}_{2,1}$ and $\tilde{u}_{2,2}$, corresponding to $x_2 \equiv 2\pi$ and initial conditions $y_2(0) \in (\Lambda_1, \Lambda_3)$ and $y_2(0) \in (\Lambda_3, \Lambda_{\max})$, respectively. They are invariant and asymptotic to P_2 .
- finite energy planes $\tilde{u}'_{3,1} = (\tilde{u}_{3,1})_\rho$ and $\tilde{u}'_{3,2} = (\tilde{u}_{3,2})_\rho$, which corresponds to $x_2 \equiv 4\pi$ and initial conditions $y_2(0) \in (\Lambda_1, \Lambda_3)$ and $y_2(0) \in (\Lambda_3, \Lambda_{\max})$, respectively. They are both asymptotic to $P'_3 = (P_3)_\rho$.

- finite energy cylinders \tilde{v}_1 and $\tilde{v}_2 = (\tilde{v}_1)_\rho$, corresponding to $y_2 \equiv \Lambda_3$ and initial conditions $x_2(0) \in (0, 2\pi)$ and $x_2(0) \in (2\pi, 4\pi)$, respectively. The cylinder \tilde{v}_1 is asymptotic to P_3 at $+\infty$ and to P_2 at $-\infty$, and \tilde{v}_2 is asymptotic to $P'_3 = (P_3)_\rho$ at $+\infty$ and to $P_2 = (P_2)_\rho$ at $-\infty$.

The following statement is taken from [12, Theorem 1.5] and [28, Theorem 4.5.44]. Note that J is not required to be generic.

Theorem 5.5 (Hofer-Wysocki-Zehnder, Wendl). *Let a closed three-manifold M be equipped with a contact form λ and a $d\lambda$ -compatible almost complex structure J . Assume that $\tilde{u} = (a, u): \mathbb{C} \rightarrow \mathbb{R} \times M$ is an embedded finite energy \tilde{J} -holomorphic plane, asymptotic to a non-degenerate periodic orbit $P = (x, T)$ having $\mu_{\text{CZ}}(P) = 3$. Then there exists an $\delta > 0$ and an embedding*

$$\tilde{\Phi}: \mathbb{R} \times (-\delta, \delta) \times \mathbb{C} \rightarrow \mathbb{R} \times M, \quad (\sigma, \tau, z) \mapsto (a_\tau(z) + \sigma, u_\tau(z)),$$

having the following properties:

- (1) For each $\sigma \in \mathbb{R}$ and $\tau \in (-\delta, \delta)$ the map $\tilde{u}_{\sigma, \tau} = \tilde{\Phi}(\sigma, \tau, \cdot)$ is up to parametrisation an embedded finite energy \tilde{J} -holomorphic plane and $\tilde{u}_{0,0} = \tilde{u}$.
- (2) The map $u_\tau(\cdot): (-\delta, \delta) \times \mathbb{C} \rightarrow M$ is an embedding and its image is disjoint from the asymptotic limit P . In particular, the maps $u_\tau: \mathbb{C} \rightarrow M$ are embeddings for all $\tau \in (-\delta, \delta)$, with mutually disjoint images that do not intersect their asymptotic limit P .
- (3) For any sequence $\tilde{u}_k = (a_k, u_k)$ of finite energy \tilde{J} -holomorphic planes such that they are all asymptotic to P and satisfy $\tilde{u}_k \rightarrow \tilde{u}$ in $C_{\text{loc}}^\infty(\mathbb{C})$ for all k sufficiently large, there exists a sequence $(\sigma_k, \tau_k) \in \mathbb{R} \times (-\delta, \delta)$ converging to $(0, 0)$ and a sequence $\varphi_k: \mathbb{C} \rightarrow \mathbb{C}$ of biholomorphic reparametrisations of \mathbb{C} of the form $z \mapsto bz + c$ with constants $b, c \in \mathbb{C}$, such that $\tilde{u}_k = \tilde{u}_{\sigma_k, \tau_k} \circ \varphi_k$.

An application of the previous theorem to the finite energy plane $\tilde{u}_{3,1}$ (recall that P_3 is non-degenerate and satisfies $\mu_{\text{CZ}}(P_3) = 3$, see Proposition 5.4) yields a maximal one-parameter family of embedded finite energy \tilde{J} -holomorphic planes

$$\tilde{u}_\tau = (a_\tau, u_\tau): \mathbb{C} \rightarrow \mathbb{R} \times \Sigma, \quad \tau \in (\tau_-, \tau_+),$$

all asymptotic to P_3 . This family is non-compact. Indeed, otherwise there is $\tau_1 \neq \tau_2$ with $u_{\tau_1}(\mathbb{C}) \cap u_{\tau_2}(\mathbb{C}) \neq \emptyset$. Then it follows from [10, Theorem 1.4] that $u_{\tau_1}(\mathbb{C}) = u_{\tau_2}(\mathbb{C})$, and hence we find an open book decomposition of Σ with binding P_3 and disc-like pages. By the usual argument, every page is transverse to the Reeb vector field, implying that every periodic orbit other than P_3 is linked to P_3 . This contradicts to the presence of P_2 and P'_3 .

We now take a look at the breaking of the family $\{\tilde{u}_\tau\}$ as $\tau \rightarrow \tau_\pm$. For simplicity we write $\tau_- = 0$ and $\tau_+ = 1$. We assume that τ strictly increases in the direction of the Reeb vector field.

Pick a sequence $\tau_n \rightarrow 0^+$ as $n \rightarrow +\infty$ and write $\tilde{u}_n := \tilde{u}_{\tau_n}$, $n \in \mathbb{N}$. By a standard argument (see [6, 14, 16]), we find that \tilde{u}_n converges to a holomorphic building with height 2. The top consists of an embedded finite energy \tilde{J} -holomorphic cylinder $\tilde{v} = (b, v): \mathbb{C} \setminus \{0\} \rightarrow \mathbb{R} \times \Sigma$ asymptotic to P_3 at its positive puncture $+\infty$ and to an index 2 orbit Q at its negative puncture 0. The bottom consists of an embedded finite energy \tilde{J} -holomorphic plane $\tilde{u} = (a, u): \mathbb{C} \rightarrow \mathbb{R} \times \Sigma$ asymptotic to Q . Moreover, given a neighbourhood $U \subset \Sigma$ of $v(\mathbb{C} \setminus \{0\}) \cup Q \cup u(\mathbb{C})$, we have $u_n(\mathbb{C}) \subset U$ for n sufficiently large. See [13] and also [6, Proposition 9.5]. Since P_2 is a unique index 2

orbit, see Proposition 5.4, we have $Q = P_2$. The uniqueness property of finite energy planes asymptotic to P_2 and finite energy cylinders asymptotic to P_3 at $+\infty$ and to P_2 at 0 (see [6, Proposition C.-3]), based on Siefring's intersection theory [27], implies that $\tilde{v} = \tilde{v}_1$ or $\tilde{v} = \tilde{v}_2$ and $\tilde{u} = \tilde{u}_{2,1}$ or $\tilde{u} = \tilde{u}_{2,2}$, up to reparametrisation and \mathbb{R} -translation.

We now choose a sequence $\tau'_n \rightarrow 1^-$ as $n \rightarrow +\infty$ and do a similar business with $\tilde{u}'_n := \tilde{u}_{\tau'_n}$. This sequence also converges to a holomorphic building with height 2 whose top level consists of an embedded finite energy cylinder $\tilde{v}' = (b', v') : \mathbb{C} \setminus \{0\} \rightarrow \mathbb{R} \times \Sigma$ asymptotic to P_3 at its positive puncture $+\infty$ and to P_2 at its negative puncture 0 and whose bottom consists of an embedded finite energy plane $\tilde{u}' = (a', u') : \mathbb{C} \rightarrow \mathbb{R} \times \Sigma$ asymptotic to P_2 . By uniqueness, we have $\tilde{v}' = \tilde{v}_1$ or $\tilde{v}' = \tilde{v}_2$ and $\tilde{u}' = \tilde{u}_{2,1}$ or $\tilde{u}' = \tilde{u}_{2,2}$, up to reparametrisation and \mathbb{R} -translation. Moreover, given a neighbourhood $U' \subset \Sigma$ of $v'(\mathbb{C} \setminus \{0\}) \cup P_2 \cup u'(\mathbb{C})$, we have $u'_n(\mathbb{C}) \subset U'$ for n sufficiently large.

Lemma 5.6. $v(\mathbb{C} \setminus \{0\}) = v'(\mathbb{C} \setminus \{0\}) = v_1(\mathbb{C} \setminus \{0\})$, $u(\mathbb{C}) = u_{2,1}(\mathbb{C})$ and $u'(\mathbb{C}) = u_{2,2}(\mathbb{C})$.

Proof. Arguing indirectly we assume that $v(\mathbb{C} \setminus \{0\}) = v_2(\mathbb{C} \setminus \{0\})$. Recall that it is obtained as the Σ -part of a limit of the sequence $\tilde{u}_{\tau_n} = (a_{\tau_n}, u_{\tau_n})$ with $\tau_n \rightarrow 0^+$. Given a neighbourhood U of $v_2(\mathbb{C} \setminus \{0\}) \cup P_2 \cup u(\mathbb{C})$, we have $u_{\tau_n}(\mathbb{C}) \subset U$ for all n sufficiently large. Since the x_2 -components of $\tilde{u}_{3,1}$, \tilde{v}_2 and \tilde{u} satisfy $x_2 \equiv 0$, $2\pi < x_2 < 4\pi$ and $x_2 \equiv 2\pi$, respectively, this implies that there is $\tau_0 \in (0, 1)$ such that u_{τ_0} admits a point with $x_2 = 2\pi$. Thus, u_{τ_0} intersects $u_{2,1}$ or $u_{2,2}$, contradicting the stability and positivity of intersections of immersed pseudoholomorphic curves (see [22, Appendix E]). We conclude that $v(\mathbb{C} \setminus \{0\}) = v_1(\mathbb{C} \setminus \{0\})$. By the same reasoning, we obtain $v'(\mathbb{C} \setminus \{0\}) = v_1(\mathbb{C} \setminus \{0\})$.

We now show that the planes u and u' are disjoint. We follow the argument given in the proof of [4, Proposition 3.17]. Assume by contradiction that they have a non-empty intersection. Then Theorem 2.4 in [27] shows that $u(\mathbb{C}) = u'(\mathbb{C})$. Pick any point $q \in \Sigma \setminus (P_3 \cup v(\mathbb{C} \setminus \{0\}) \cup P_2 \cup u(\mathbb{C}))$ and take a small neighbourhood \mathcal{U} of $P_3 \cup v(\mathbb{C} \setminus \{0\}) \cup P_2 \cup u(\mathbb{C})$, not containing q . Then there exists τ_0 and τ_1 contained in $(0, 1)$, close enough to 0 and 1, respectively, such that $u_{\tau_0}(\mathbb{C}), u_{\tau_1}(\mathbb{C}) \subset \mathcal{U}$. By Jordan-Brouwer separation theorem, the piecewise smooth embedded two-sphere $S = u_{\tau_0}(\mathbb{C}) \cup P_3 \cup u_{\tau_1}(\mathbb{C})$ divides Σ into two components C_1 and C_2 having boundary S . It follows from the choice of the point q that one of the two components, say C_1 , contains q in its interior and the other contains $P_3 \cup v(\mathbb{C} \setminus \{0\}) \cup P_2 \cup u(\mathbb{C})$.

We claim that the set $A = \left(\bigcup_{\tau \in (0,1)} u_{\tau}(\mathbb{C}) \right) \cap \text{int}(C_1)$ is non-empty, open and closed in $\text{int}(C_1)$. In view of Theorem 5.5 it is non-empty and open. In order to achieve the closedness of A , take a sequence $w_n \in A$. Since w_n is contained the closed subset C_1 , a limit of the sequence w_n is contained in C_1 . On the other hand, since w_n is also contained in the union $\bigcup_{\tau \in (0,1)} u_{\tau}(\mathbb{C})$, the compactness property of the family $\{u_{\tau}\}_{\tau \in (0,1)}$ described above implies that its limit is contained either in $\bigcup_{\tau \in (0,1)} u_{\tau}(\mathbb{C})$, in P_3 , or in $v(\mathbb{C} \setminus \{0\}) \cup P_2 \cup u(\mathbb{C})$. The last option does not occur because $v(\mathbb{C} \setminus \{0\}) \cup P_2 \cup u(\mathbb{C})$ is contained in the interior of C_2 . Therefore, a limit of the sequence w_n is contained in $\left(\bigcup_{\tau \in (0,1)} u_{\tau}(\mathbb{C}) \cup P_3 \right) \cap C_1$, from which we see that the set $\left(\bigcup_{\tau \in (0,1)} u_{\tau}(\mathbb{C}) \cup P_3 \right) \cap C_1$ is closed in Σ . This proves the claim.

The claim above implies that $q \in \bigcup_{\tau \in (0,1)} u_\tau(\mathbb{C})$. It follows from the choice of q that

$$\Sigma = P_3 \cup v(\mathbb{C} \setminus \{0\}) \cup P_2 \cup u(\mathbb{C}) \cup \bigcup_{\tau \in (0,1)} u_\tau(\mathbb{C}),$$

and hence there exists $\tau_0 \in (0, 1)$ such that u_{τ_0} admits a point with $x_2 = 2\pi$, which derives a contradiction as above. Consequently, we find $u(\mathbb{C}) \cap u'(\mathbb{C}) = \emptyset$. Since τ increases in the direction of the Reeb vector field, we have $u(\mathbb{C}) = u_{2,1}(\mathbb{C})$ and $u'(\mathbb{C}) = u_{2,2}(\mathbb{C})$. This completes the proof. \square

Abbreviate

$$\mathfrak{B} = \{(x_1, x_2, y_1, y_2) \in \Sigma \mid x_2 \leq 2\pi\},$$

whose boundary is the piecewise smooth embedded two-sphere $u_{2,1}(\mathbb{C}) \cup P_2 \cup u_{2,2}(\mathbb{C})$. The proof of the previous lemma shows that the images of the planes $u_{2,1}, u_{2,2}$ and $u_\tau, \tau \in (0, 1)$ and the cylinder v_1 determine a smooth foliation of $\mathfrak{B} \setminus (P_2 \cup P_3)$. Since the finite energy plane $\tilde{u}_{3,2}$ corresponds to $x_2 \equiv 0$, we have $u_{3,2}(\mathbb{C}) \subset \mathfrak{B} \setminus (P_2 \cup P_3)$. Therefore, there is $\tau_* \in (0, 1)$ such that $u_{\tau_*}(\mathbb{C}) \cap u_{3,2}(\mathbb{C}) \neq \emptyset$. We find again by [10, Theorem 1.4] that $u_{\tau_*}(\mathbb{C}) = u_{3,2}(\mathbb{C})$.

Note that

$$\rho(\mathfrak{B}) = \overline{\Sigma \setminus \mathfrak{B}} = \{(x_1, x_2, y_1, y_2) \in \Sigma \mid x_2 \geq 2\pi\}.$$

We then push all the data above to the region $\rho(\mathfrak{B})$. More precisely, we have a one-parameter family of embedded finite energy \tilde{J} -holomorphic planes

$$(\tilde{u}_\tau)_\rho: \mathbb{C} \rightarrow \mathbb{R} \times \Sigma, \quad \tau \in (\tau_-, \tau_+),$$

all asymptotic to $P'_3 = \rho(P_3)$. Note that $(u_{\tau_*})_\rho(\mathbb{C}) = u'_{3,2}(\mathbb{C})$. This family breaks onto $\tilde{v}_2 = (\tilde{v}_1)_\rho$ and $\tilde{u}_{2,1} = (\tilde{u}_{2,1})_\rho$ at one end and onto \tilde{v}_2 and $\tilde{u}_{2,2} = (\tilde{u}_{2,2})_\rho$ at the other end. The images of maps $u_{2,1}, u_{2,2}, (u_\tau)_\rho, \tau \in (\tau_-, \tau_+)$ and v_2 fill the three-ball $\rho(\mathfrak{B})$.

We have constructed a stable finite energy foliation $\tilde{\mathcal{F}}$ of $\mathbb{R} \times \Sigma$, which is symmetric with respect to the exact anti-symplectic involution $\tilde{\rho}$ and whose leaves are embedded finite energy planes and cylinders. Denote by \mathcal{F} the projection of $\tilde{\mathcal{F}}$ to Σ , which is symmetric with respect to the anti-contact involution ρ . Since finite energy planes in $\tilde{\mathcal{F}}$ are asymptotic to P_2 or P_3 , their Σ -projections are transverse to the Reeb vector field [15]. See also [8, Section 13.6]. It is straightforward to see that the Σ -parts v_1, v_2 of the cylinders \tilde{v}_1, \tilde{v}_2 are transverse to the Reeb vector field as well. Therefore, \mathcal{F} determines a transverse foliation of Σ whose binding orbits are P_2, P_3 and P'_3 and whose regular leaves are embedded planes and cylinders. See Figure 9.

Remark 5.7. A transverse foliation satisfying the properties above is called a weakly convex foliation. For more details, see [5].

We now cut the energy level Σ along the two-spheres

$$\begin{aligned} B &= \{(x_1, x_2, y_1, y_2) \in \Sigma \mid x_2 = 0\} = u_{3,1}(\mathbb{C}) \cup P_3 \cup u_{3,2}(\mathbb{C}), \\ \rho(B) &= \{(x_1, x_2, y_1, y_2) \in \Sigma \mid x_2 = 4\pi\} = u'_{3,1}(\mathbb{C}) \cup P'_3 \cup u'_{3,2}(\mathbb{C}). \end{aligned}$$

Denote by Σ_0 a unique component whose boundary is given by $B \cup \rho(B)$. It is diffeomorphic to $S^2 \times I$, where I is a closed interval. We then identify B and $\rho(B)$, providing us with $\bar{\Sigma} \cong S^2 \times S^1$. Recall that $\bar{\Sigma}$ is a unique connected component of $\bar{H}^{-1}(c)$ which contains $\bar{\Sigma}_{\text{direct}}^u$, the double cover of Σ_{direct}^u . See Section 5.2. The

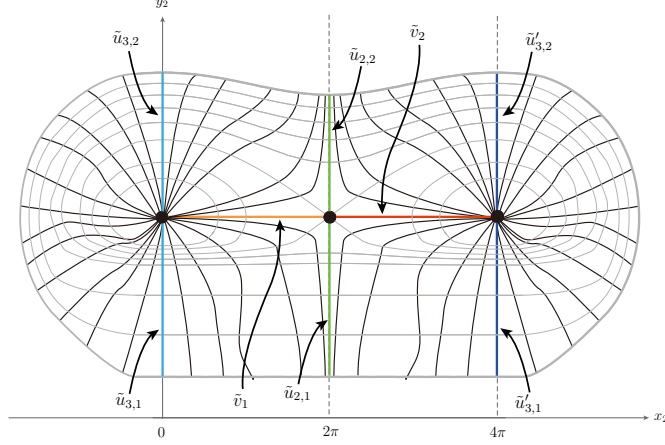


FIGURE 9. The projection of the transverse foliation \mathcal{F} to the (x_2, y_2) -plane. The black curves indicate the families of planes.

contact form λ , constructed in Section 5.3, induces a contact form $\bar{\lambda}$ on $\bar{\Sigma}$, and the anti-contact involution ρ induces an anti-contact involution on the contact manifold $(\bar{\Sigma}, \bar{\lambda})$. We denote it again by ρ . The unique index-2 periodic orbit P_2 still lies on $\bar{\Sigma}$, and the two index-3 binding orbits P_3 and P'_3 now provide a single symmetric periodic index-3 orbit, still denoted by P_3 . The periodic orbit P_0 yields two periodic orbits, one satisfies $y_2 = \Lambda_{\max}$ and the other satisfies $y_2 \equiv \Lambda_1$. Note that the latter is the second iterate of the direct circular orbit γ_{direct}^u .

The almost complex structure $J: \xi \rightarrow \xi$ as in (5.11) induces a $d\bar{\lambda}$ -compatible and ρ -anti-invariant almost complex structure $\bar{J}: \bar{\xi} \rightarrow \bar{\xi}$, where $\bar{\xi} = \ker \bar{\lambda}$. Hence, the finite energy foliation $\bar{\mathcal{F}}$ of $\mathbb{R} \times \bar{\Sigma}$ induces a finite energy foliation of $\mathbb{R} \times \bar{\Sigma}$ consisting of the following:

- finite energy planes $\tilde{u}_{3,1}$ and $\tilde{u}_{3,2}$, corresponding to $x_2 \equiv 0 \pmod{4\pi}$ and initial conditions $y_2(0) \in (\Lambda_1, \Lambda_3)$ and $y_2(0) \in (\Lambda_3, \Lambda_{\max})$, respectively. They satisfy $\tilde{u}_{3,j} = (\tilde{u}_{3,j})_\rho, j = 1, 2$ and are both asymptotic to P_3 .
- finite energy planes $\tilde{u}_{2,1}$ and $\tilde{u}_{2,2}$, corresponding to $x_2 \equiv 2\pi \pmod{4\pi}$ and initial conditions $y_2(0) \in (\Lambda_1, \Lambda_3)$ and $y_2(0) \in (\Lambda_3, \Lambda_{\max})$, respectively. They satisfy $\tilde{u}_{2,j} = (\tilde{u}_{2,j})_\rho, j = 1, 2$ and are both asymptotic to P_2 .
- finite energy cylinders \tilde{v}_1 and $\tilde{v}_2 = (\tilde{v}_1)_\rho$, which corresponds to $y_2 \equiv \Lambda_3$ and initial conditions $x_2(0) \in (0, 2\pi)$ and $x_2(0) \in (2\pi, 4\pi)$, respectively. They are both asymptotic to P_3 at $+\infty$ and to P_2 at $-\infty$.
- two families of finite energy planes $(\tilde{u}_{j,\tau}), \tau \in (0, 1)$. For each $j = 1, 2$, the family $(\tilde{u}_{j,\tau})$ breaks onto \tilde{v}_1 and $\tilde{u}_{2,j}$ at one end and onto \tilde{v}_2 and $\tilde{u}_{2,j}$ at the other end.

The projection of the finite energy foliation above defines a transverse foliation $\bar{\mathcal{F}}$ of $\bar{\Sigma}$, whose binding orbits are P_2 and P_3 and whose regular leaves are embedded planes and cylinders.

Denote by \mathcal{T} the compact subset of the energy level $\bar{\Sigma}$, which projects into the (x_2, y_2) -plane (modulo 4π in x_2) as the set

$$\{(x_2, y_2) \mid x_2 \in \mathbb{R}/4\pi\mathbb{Z}, \Lambda_1 \leq y_2 \leq \Lambda_3\}.$$

Note that the double cover $\bar{\Sigma}_{\text{direct}}^u$ of the set Σ_{direct}^u under consideration is contained in \mathcal{T} and that \mathcal{T} is diffeomorphic to a solid torus and has boundary

$$\partial\mathcal{T} = P_3 \cup P_2 \cup v_1(\mathbb{C} \setminus \{0\}) \cup v_2(\mathbb{C} \setminus \{0\})$$

lying over the set $\{(x_2, \Lambda_3) \mid x_2 \in \mathbb{R}/4\pi\mathbb{Z}\}$. The interior of \mathcal{T} is filled with the images of planes $u_{2,1}$ and $u_\tau = u_{1,\tau}, \tau \in (0, 1)$. The core of this solid torus is the second iterate of the direct circular orbit γ_{direct}^u .

Let $F \in \bar{\mathcal{F}}$ be a plane asymptotic to P_3 that is not rigid and contained in \mathcal{T}_1 . For $j = 1, 2$, denote $\Pi_j(x_1, x_2, y_1, y_2) = (x_j, y_j), (x_1, x_2, y_1, y_2) \in \bar{\Sigma}$. Then $\Pi_1(F)$ is a closed disc of radius r_3 centred at the origin and $\Pi_2(F)$ is an arc connecting (x_2, Λ_1) for some $x_2 \in (0, 4\pi)$ and $(0, \Lambda_3) \equiv (4\pi, \Lambda_3)$. If $(x_1, x_2, y_1, y_2) \in \bar{\Sigma}$ is such that $(x_2, y_2) \in \Pi_2(F)$ with $y_2 < \Lambda_2$, then (x_1, y_1) lies along the circle

$$x_1^2 + y_1^2 = 2 \left(c + \frac{1}{2y_2^2} + y_2 \right). \quad (5.26)$$

See (5.1). Note that the right-hand side above equals zero if and only if $y_2 = \Lambda_1$.

In order to show that $\bar{\mathcal{F}}$ intersects the set $\bar{\Sigma}_{\text{direct}}^u$ in embedded discs, we have to rule out the presence of a regular leaf $F \in \bar{\mathcal{F}}$ having the property that there is $y_2 < \Lambda_2$ such that $\#\left[\Pi_2(F) \cap \{(x_2, y_2) \mid 0 < x_2 < 4\pi\}\right] > 1$, as illustrated in Figure 10. To this end, fix a regular leaf $F \in \bar{\mathcal{F}}$, asymptotic to P_3 and contained

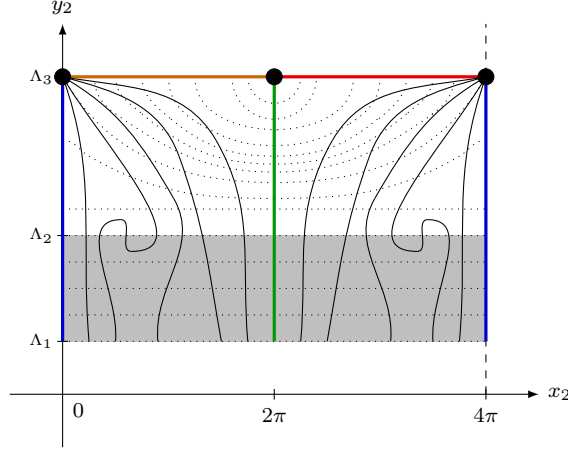


FIGURE 10. An unpleasant scenario that is not the case.

in $\mathcal{T} \setminus \partial\mathcal{T}$. Let $\tilde{u} = (a, u)$ be a corresponding finite energy plane. Denote $u(s, t) = (x_1(s, t), x_2(s, t), y_1(s, t), y_2(s, t))$ as before. Assume by contradiction that there is (s_0, t_0) such that $\Lambda_1 < y_2(s_0, t_0) \leq \Lambda_2$ and $(y_2)_s(s_0, t_0) = (y_2)_t(s_0, t_0) = 0$. Introduce polar coordinates (r, ϑ) in the (x_1, y_1) -plane. By means of (5.26) we find that

$$r(s, t)r_\sigma(s, t) = -(y_2)_\sigma(s, t) \left(\frac{1}{y_2(s, t)^3} - 1 \right), \quad \sigma = s, t.$$

Since $y_2(s_0, t_0) > \Lambda_1 > 1$, we find $r(s_0, t_0) > 0$, and hence $r_s(s_0, t_0) = r_t(s_0, t_0) = 0$. Let $\gamma(t) = (x_1(t), x_2(t), y_1(t), y_2(t))$ be a Hamiltonian trajectory that intersects F at $u(s_0, t_0)$. Since $y_2 \leq \Lambda_2$, without loss of generality we may assume that $\bar{H} = H$, where the latter is as in (5.1). Since H is free of the variable x_2 , we find using

Hamilton's equations that $y_2(t) = y_2(s_0, t_0), \forall t$. Moreover, $\Pi_1(\gamma(t))$ moves along the circle of radius $r(s_0, t_0)$. The discussion so far shows that F and γ have a non-empty tangent intersection at $u(s_0, t_0)$, contradicting the fact that F is transverse to the Hamiltonian flow.

It remains to show that the associated first return map admits a unique fixed point corresponding to the direct circular orbit γ_{direct}^u . It is obvious that γ_{direct}^u corresponds to a fixed point. Recall that every periodic orbit $\gamma \neq \gamma_{\text{direct}}^u$ in Σ_{direct}^u is a $T_{k,l}$ -type orbit for some coprime positive integers k, l . See Section 3. It is easy to see that $k < l$ on Σ_{direct}^u . See for instance [2, Section 6] or [18, Section 3]. This implies that the periods of $\Pi_1\gamma$ and $\Pi_2\gamma$ do not coincide, and hence every $T_{k,l}$ -type orbit intersects each leaf at least twice.

We conclude that the transverse foliation $\bar{\mathcal{F}}$ of $\bar{\Sigma}$ intersects Σ_{direct}^u in embedded discs, providing a disc foliation of Σ_{direct}^u . Moreover, the associated first return map has a unique fixed point corresponding to γ_{direct}^u . This finishes the proof of Theorem 1.1 for energies below the critical value.

Remark 5.8. In Appendix A we will embed Σ_{direct}^u into a closed three-manifold $\hat{\Sigma} \cong S^2 \times S^1$ and then construct its finite energy foliation, projecting to an open book decomposition of $\hat{\Sigma}$ with annulus-like pages. The intersection of this open book decomposition with Σ_{direct}^u provides a foliation of Σ_{direct}^u into annuli, whose inner boundaries are the direct circular orbit γ_{direct}^u and the outer boundaries lie on the boundary torus $\partial\Sigma_{\text{direct}}^u$. The construction is explicit and does not require the implicit function theorem and compactness argument.

6. ABOVE THE CRITICAL ENERGY

Fix $-\frac{3}{2} < c < 0$ and let $E_0 \in (E_{\text{retro}}^u, c)$. Recall that $E = c$ corresponds to the collision orbits. This section is devoted to prove the assertion of Theorem 1.1 for the set

$$\Sigma_{\text{retro}}^u = \{\text{all periodic orbits of } X_H \text{ with } E \in [E_{\text{retro}}^u, E_0]\} \subset \Sigma_c^u,$$

which is diffeomorphic to a solid torus with core being the retrograde circular orbit γ_{retro}^u . Note that it contains only retrograde orbits and no collision orbits.

In this case the transformed Hamiltonian is given by

$$H(x_1, x_2, y_1, y_2) = -\frac{1}{2y_2^2} - y_2 - \frac{1}{2}(x_1^2 + y_1^2)$$

for $(x_1, x_2, y_1, y_2) \in \bar{\mathcal{P}}' \subset \mathbb{R} \times \mathbb{R}/2\pi\mathbb{Z} \times \mathbb{R} \times \mathbb{R}_-$. For convenience, we shall work with $-H$ instead of H , so that every orbit is oriented in the opposite direction. Note that the qualitative behaviour of the dynamics does not change. By abuse of notation, we denote $-H$ again by H , namely, we have

$$\begin{aligned} H(x_1, x_2, y_1, y_2) &= \frac{1}{2y_2^2} + y_2 + \frac{1}{2}(x_1^2 + y_1^2) \\ &= H_1(x_1, y_2) - H_2(y_2), \end{aligned}$$

where H_1 and H_2 are as in (5.2). Note that

$$y_2 \in [\nu_2, \nu_1] \quad \text{on } \Sigma_{\text{retro}}^u,$$

where $\nu_1 = -\sqrt{-\frac{1}{2E_{\text{retro}}^u}} \in (-\frac{1}{\sqrt{2}}, -\frac{1}{2})$ and $\nu_2 = -\sqrt{-\frac{1}{2E_0}}$.

Arguing as in Section 5.1 one can construct a disc foliation of Σ_{retro}^u by looking at the negative gradient flow lines of $-H_2$. See Figure 11. Let h_{x_2} be the negative

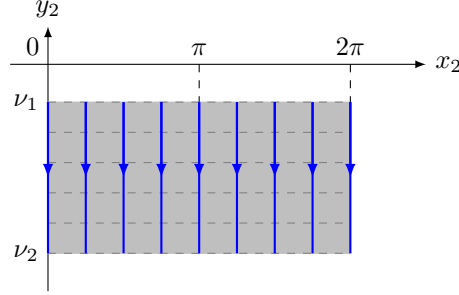


FIGURE 11. Negative gradient flow lines of $-H_2$. Dashed lines indicate Hamiltonian trajectories.

gradient flow line of $-H_2$ corresponding to $x_2 \in \mathbb{R}/2\pi\mathbb{Z}$. Its preimage $\Pi^{-1}(h_{x_2})$ under the projection $\Pi(x_1, x_2, y_1, y_2) = (x_2, y_2)$, $(x_1, x_2, y_1, y_2) \in \Sigma_{\text{retro}}^u$ is an embedded disc, transverse to the Hamiltonian flow. By varying x_2 in $\mathbb{R}/2\pi\mathbb{Z}$, we find a disc foliation of Σ_{retro}^u .

Fix $\nu_3 \in (-\infty, \nu_2)$ and $0 < \varepsilon_0 < \frac{1}{2}(\nu_2 - \nu_3)$. Consider

$$U(x_2, y_2) = \frac{1}{2}(y_2 - \nu_3)^2 - \cos \frac{x_2}{2} + D,$$

where $(x_2, y_2) \in \mathbb{R}/4\pi\mathbb{Z} \times \mathbb{R}_+$, and D is a constant satisfying

$$D < \min\left\{0, \frac{1}{2(\nu_2 - \varepsilon_0)^2} + (\nu_2 - \varepsilon_0) - \frac{1}{2}(\nu_2 - \varepsilon_0 - \nu_3)^2 - 1\right\}.$$

Set

$$V(x_2, y_2) = -(1 - f(y_2))H_2(y_2) + f(y_2)U(x_2, y_2),$$

where a non-increasing smooth function $f: \mathbb{R} \rightarrow [0, 1]$ satisfies $f(y_2) = 1, \forall y_2 < \nu_2 - 2\varepsilon_0$ and $f(y_2) = 0, \forall y_2 > \nu_2 - \varepsilon_0$. See Figure 12. Because of the choice of the constant D , we have

$$V_{y_2} < 0, \forall y_2 < \nu_3 \quad \text{and} \quad V_{y_2} > 0, \forall y_2 < \nu_3,$$

and $(0, \nu_3)$ and $(2\pi, \nu_3)$ are the only critical points of V . Given x_2 , denote by $\nu_{\min} = \nu_{\min}(x_2)$ the value of y_2 satisfying $V(x_2, \nu_{\min}) = -c$.

We define

$$\bar{H}(x_1, x_2, y_1, y_2) = H_1(x_1, y_1) + V(x_2, y_2),$$

where $(x_2, y_2) \in \mathbb{R}/4\pi\mathbb{Z} \times \mathbb{R}_+$, and note that it is invariant under the anti-symplectic involution ρ as in (5.5).

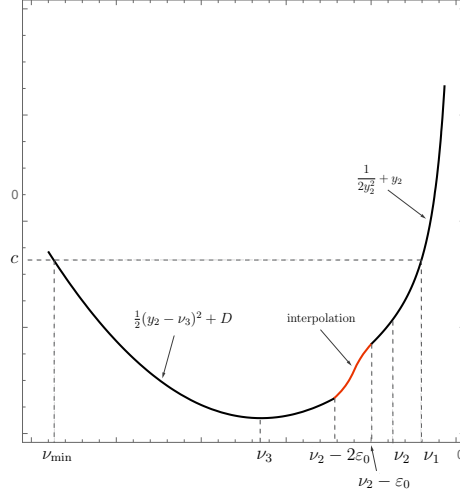
We now break the periodicity in x_2 precisely as in Section 5.2. Namely, we consider

$$W(x_2, y_2) = \frac{1}{2}x_2^2 + \frac{1}{2}(y_2 - \nu_3)^2$$

and interpolate

$$\tilde{V}(x_2, y_2) = ((1 - g(x_2))W(x_2, y_2) + g(x_2)V(x_2, y_2)),$$

where g is a non-decreasing smooth function $g: \mathbb{R} \rightarrow [0, 1]$ such that $g(x_2) = 0, \forall x_2 < -2\varepsilon_1$ and $g(x_2) = 1, \forall x_2 > -\varepsilon_1$ with $\varepsilon_1 > 0$ small enough. By repeating

FIGURE 12. Interpolation for variable y_2

in a similar manner for $x_2 \geq 2\pi$ in a symmetric way, we obtain a smooth function $\tilde{H}_2(x_2, y_2)$. Note that it is symmetric in x_2 with respect to $x_2 = 2\pi$.

We then obtain a modified Hamiltonian

$$\tilde{H}(x_1, x_2, y_1, y_2) = H_1(x_1, y_1) + \tilde{H}_2(x_2, y_2).$$

It is easy to see that \tilde{H} admits exactly three critical points given in (5.7) and satisfies

$$\tilde{H}_{y_2} < 0, \quad \forall y_2 < \nu_3, \quad \tilde{H}_{y_2} > 0, \quad \forall y_2 > \nu_3.$$

This implies that there is a connected component $\Sigma \cong S^3$ of the energy level $\tilde{H}^{-1}(-c)$. The anti-symplectic involution ρ induces an anti-symplectic involution of $\mathbb{R}^3 \times \mathbb{R}_-$, still denoted by ρ . Since \tilde{H} is invariant under ρ , so is Σ .

The rest of the proof is analogous to the previous case, so we omit it. This finishes the proof.

ACKNOWLEDGMENTS

The author would like to express his gratitude to Urs Frauenfelder and Pedro Salomão for invaluable comments. He was supported by the National Research Foundation of Korea(NRF) grant funded by the Korea government(MSIT) (No. NRF-2022R1F1A1074066).

APPENDIX A. ANNULUS FOLIATIONS

As announced in Remark 5.8 we shall construct a foliation of Σ_{direct}^u (when $c < -\frac{3}{2}$) different from the one given in Section 5. An annulus foliation of Σ_{retro}^u (when $c \in (-\frac{3}{2}, 0)$) can be constructed in a similar manner.

We fix $c < -\frac{3}{2}$ and $E_0 \in (E_{\text{direct}}^u, 0)$ and define $\Sigma_{\text{direct}}^u \subset \Sigma_c^u$ as before. Consider $\Lambda_3 > \Lambda_2$ and $0 < \varepsilon < \frac{1}{2}(\Lambda_3 - \Lambda_2)$, where Λ_2 is as in Section 5. Let

$$V(y_2) = \frac{1}{2}(y_2 - \Lambda_3)^2 + B,$$

where the constant B is given as in (5.3), and define

$$\hat{H}_2(y_2) = (1 - f(y_2))H_2(y_2) + f(y_2)V(y_2),$$

where $f: \mathbb{R} \rightarrow [0, 1]$ is a non-decreasing function satisfying

$$\begin{cases} f(y_2) = 0 & y_2 < \Lambda_2 + \varepsilon, \\ f(y_2) = 1 & y_2 > \Lambda_2 + 2\varepsilon. \end{cases}$$

Arguing as in Section 5.2, we see that

$$\hat{H}'_2 < 0, \quad \forall y_2 < \Lambda_3 \quad \text{and} \quad \hat{H}'_2 > 0, \quad \forall y_2 > \Lambda_3. \quad (\text{A.1})$$

We introduce

$$\hat{H}(x_1, x_2, y_1, y_2) = H_1(x_1, y_1) + \hat{H}_2(y_2).$$

Note that \hat{H} is free of the variable x_2 . The energy level $\hat{H}^{-1}(c)$ contains a connected component $\hat{\Sigma} \cong S^1 \times S^2$, containing Σ_{direct}^u , where we have identified $S^1 \cong \mathbb{R}/2\pi\mathbb{Z}$. If $(x_1, x_2, y_1, y_2) \in \hat{\Sigma}$, then

$$\Lambda_1 \leq y_2 \leq \Lambda_{\max} := \sqrt{2(c - B)} + \Lambda_3.$$

The Liouville vector field

$$\hat{Y} = \frac{1}{2}(x_1\partial_{x_1} + y_1\partial_{y_1}) + (y_2 - \Lambda_3)\partial_{y_2}$$

satisfies $d\hat{H}(\hat{Y}) > 0$, implying that it is transverse to $\hat{\Sigma}$. Therefore, we obtain a contact form $\hat{\lambda}$

$$\hat{\lambda} = \omega_0(\hat{Y}, \cdot)|_{\hat{\Sigma}} = \frac{1}{2}(y_1 dx_1 - x_1 dy_1) + (y_2 - \Lambda_3) dx_2.$$

Consider the periodic orbits $Q_1 = (w_1, T_1)$ and $Q_2 = (w_2, T_2)$, where

$$\begin{aligned} w_1(t) &= (0, (\frac{1}{\Lambda_1^3} - 1)t, 0, \Lambda_1), & T_1 &= \frac{2\pi}{1 - 1/\Lambda_1^3} \\ w_2(t) &= (0, \sqrt{2(c - B)}t, 0, \Lambda_{\max}), & T_2 &= \frac{2\pi}{\sqrt{2(c - B)}}. \end{aligned}$$

Note that Q_1 corresponds to the direct circular orbit γ_{direct}^u . Since

$$\lambda(X_{\hat{H}}) = \begin{cases} (\Lambda_1 - \Lambda_3)(\frac{1}{\Lambda_1^3} - 1) & \text{along } Q_1, \\ 2(c - B) & \text{along } Q_2, \end{cases}$$

their Reeb periods are $2\pi(\Lambda_3 - \Lambda_1)$ and $2\pi\sqrt{2(c - B)}$, respectively.

Introduce polar coordinates (r, ϑ) in the (x_1, y_1) -plane. Note that $r = \sqrt{2(c - \hat{H}_2)}$, showing that the variable r takes the minimum $r = 0$ when $\hat{H}_2 = c$, or equivalently, $y_2 \in \{\Lambda_1, \Lambda_{\max}\}$, and the maximum $r = r_{\max}$ when $y_2 = \Lambda_3$. Fix $\vartheta \in \mathbb{R}/2\pi\mathbb{Z}$ and consider $u_{\vartheta}(s) = (r(s) \cos \vartheta, r(s) \sin \vartheta)$ such that $r(s)$ satisfies

$$\lim_{s \rightarrow \pm\infty} r(s) = 0, \quad r(0) = r_{\max}.$$

Denote $\Pi(x_1, x_2, y_1, y_2) = (x_1, y_1)$. Then $\Pi^{-1}(u_{\vartheta})$ is an embedded annulus in Σ that is transverse to the Hamiltonian flow and asymptotic to Q_1 and Q_2 . By varying $\vartheta \in \mathbb{R}/2\pi\mathbb{Z}$, we obtain an open book decomposition of Σ with annulus-like pages. Each annulus, restricted to the (x_1, y_1, y_2) -space, is an arc asymptotic to the points $(0, 0, \Lambda_1)$ and $(0, 0, \Lambda_{\max})$ that correspond to the binding orbits Q_1 and Q_2 , respectively. See Figure 13.

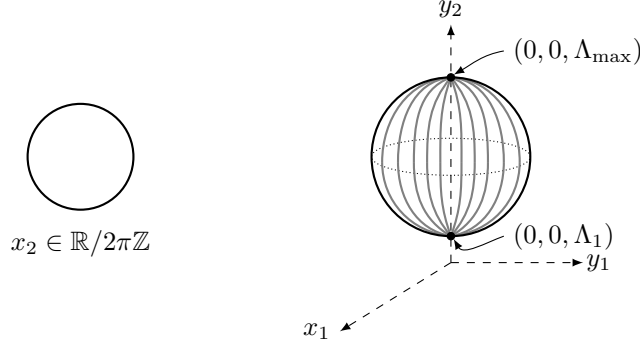


FIGURE 13. An open book decomposition of Σ with annulus-like pages

In order to construct a finite energy foliation of $\hat{\Sigma}$ projecting to the above-described open book decomposition, choose J as in Section 5.6. We fix $\vartheta \in \mathbb{R}/2\pi\mathbb{Z}$ and let $\tilde{w}_\vartheta = (d_\vartheta, w_\vartheta): \mathbb{R} \times S^1 \rightarrow \mathbb{R} \times \Sigma$ be a \tilde{J} -holomorphic curve. We make the following Ansatz:

Ansatz. The Σ -part w_ϑ is of the form

$$w_\vartheta(s, t) = (r(s) \cos \vartheta, 2\pi t, r(s) \sin \vartheta, y_2(s)),$$

where $r(s)$ satisfies $\lim_{s \rightarrow \pm\infty} r(s) = 0$.

In view of $\hat{H} = c$, we find

$$\frac{1}{2}r(s)^2 + \hat{H}_2(y_2(s)) = c. \quad (\text{A.2})$$

Proceeding as before, we find

$$\dot{y}_2(s) = \frac{2\pi r(s)^2}{r(s)^2 + \hat{H}'_2(y_2(s))^2} = \frac{4\pi(c - \hat{H}_2(y_2(s)))}{2(c - \hat{H}_2(y_2(s))) + \hat{H}'_2(y_2(s))^2}, \quad (\text{A.3})$$

which might be seen as a differential equation of type

$$\dot{y}_2(s) = P(y_2(s)).$$

Here, $P = P(y_2)$ is a smooth function on $[\Lambda_1, \Lambda_{\max}]$, which vanishes precisely at $y_2 = \Lambda_1, \Lambda_{\max}$. Since $P(y_2) > 0, \forall y_2 \in (\Lambda_1, \Lambda_{\max})$, we conclude that a solution $y_2 = y_2(s)$ to ODE (A.3) with initial condition $y_2(0) \in (\Lambda_1, \Lambda_{\max})$ is strictly increasing and satisfies

$$\lim_{s \rightarrow -\infty} y_2(s) = \Lambda_1, \quad \lim_{s \rightarrow +\infty} y_2(s) = \Lambda_{\max}.$$

We now find using (A.2) and (A.3) that

$$\dot{r}(s) = -\frac{2\pi r(s)\hat{H}'_2(y_2(s))}{r(s)^2 + \hat{H}'_2(y_2(s))^2} = \begin{cases} \sqrt{(2\pi - \dot{y}_2(s))\dot{y}_2(s)} & \text{if } \hat{H}'_2(y_2(s)) \leq 0, \\ -\sqrt{(2\pi - \dot{y}_2(s))\dot{y}_2(s)} & \text{if } \hat{H}'_2(y_2(s)) > 0. \end{cases}$$

In view of (A.1), we conclude that $r = r(s)$ is increasing for $s \in (-\infty, s_0)$ and decreasing for $s \in (s_0, +\infty)$, where s_0 denotes the time at which $y_2(s_0) = \Lambda_3$. In particular, $r(s) \rightarrow 0$ as $s \rightarrow \pm\infty$.

We also find

$$(d_{\vartheta})_s = \hat{\lambda}((w_{\vartheta})_t) = 2\pi(y_2 - \Lambda_3), \quad (d_{\vartheta})_t = \hat{\lambda}((w_{\vartheta})_s) = 0.$$

This implies that d is independent of t , and hence we may write

$$d_{\vartheta}(s, t) = 2\pi \int_0^s (y_2(u) - \Lambda_3) du.$$

Note that $d_{\vartheta}(s, t) \rightarrow +\infty$ as $s \rightarrow \pm\infty$.

We have constructed a finite energy \tilde{J} -holomorphic cylinder $\tilde{w}_{\vartheta} = (d_{\vartheta}, w_{\vartheta}): \mathbb{R} \times S^1 \rightarrow \mathbb{R} \times \Sigma$ that is asymptotic to Q_1 and Q_2 at $\mp\infty$, respectively. Note that both asymptotic limits are positive. Its Hofer energy equals the sum of the Reeb periods of Q_1 and Q_2 .

Since the above argument is independent of the choice of $\vartheta \in \mathbb{R}/2\pi\mathbb{Z}$, by varying ϑ we obtain a finite energy foliation of $\mathbb{R} \times \hat{\Sigma}$, which projects the open book decomposition of $\hat{\Sigma}$ with annulus-like pages, described above. Its intersection with the set Σ_{direct}^u yields the desired annulus foliation. Namely, the solid torus Σ_{direct}^u is foliated into annuli transverse to the Hamiltonian flow restricted to Σ_{direct}^u . The outer boundary of each annulus lies on the boundary torus $\partial\Sigma_{\text{direct}}^u$. The inner boundary coincides with the direct circular orbit γ_{direct}^u .

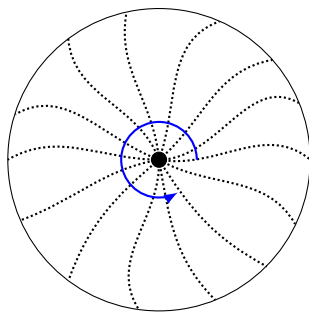


FIGURE 14. A slice of the annulus foliation. The dot and the dotted curves correspond to the direct circular orbit and annuli, respectively. The blue curve points in the direction of the Hamiltonian flow.

REFERENCES

- [1] R. Abraham and J. E. Marsden. *Foundations of mechanics*. Benjamin/Cummings Publishing Co., Inc., Advanced Book Program, Reading, Mass., 1978. Second edition, revised and enlarged, With the assistance of Tudor Rațiu and Richard Cushman.
- [2] P. Albers, J. W. Fish, U. Frauenfelder, and O. van Koert. The Conley-Zehnder indices of the rotating Kepler problem. *Math. Proc. Cambridge Philos. Soc.*, 154(2):243–260, 2013.
- [3] P. Albers, U. Frauenfelder, O. van Koert, and G. P. Paternain. Contact geometry of the restricted three-body problem. *Comm. Pure Appl. Math.*, 65(2):229–263, 2012.
- [4] C. L. de Oliveira. 3–2–1 foliations for Reeb flows on the tight 3–sphere. *arXiv preprint*, 2021.
- [5] N. V. de Paulo, U. L. Hryniewicz, S. Kim, and P. A. S. Salomão. Genus zero transverse foliations for weakly convex Reeb flows on the tight 3–sphere. *preprint*, 2022.
- [6] N. V. de Paulo and P. A. S. Salomão. Systems of transversal sections near critical energy levels of Hamiltonian systems in \mathbb{R}^4 . *Mem. Amer. Math. Soc.*, 252(1202):v+105, 2018.
- [7] U. Frauenfelder and J. Kang. Real holomorphic curves and invariant global surfaces of section. *Proc. Lond. Math. Soc. (3)*, 112(3):477–511, 2016.

- [8] U. Frauenfelder and O. van Koert. *The restricted three-body problem and holomorphic curves*. Pathways in Mathematics. Birkhäuser/Springer, Cham, 2018.
- [9] H. Hofer. Pseudoholomorphic curves in symplectizations with applications to the Weinstein conjecture in dimension three. *Invent. Math.*, 114(3):515–563, 1993.
- [10] H. Hofer, K. Wysocki, and E. Zehnder. Properties of pseudo-holomorphic curves in symplectisations. II. Embedding controls and algebraic invariants. *Geom. Funct. Anal.*, 5(2):270–328, 1995.
- [11] H. Hofer, K. Wysocki, and E. Zehnder. Properties of pseudoholomorphic curves in symplectisations. I. Asymptotics. *Ann. Inst. H. Poincaré Anal. Non Linéaire*, 13(3):337–379, 1996.
- [12] H. Hofer, K. Wysocki, and E. Zehnder. Properties of pseudoholomorphic curves in symplectizations. III. Fredholm theory. In *Topics in nonlinear analysis*, volume 35 of *Progr. Nonlinear Differential Equations Appl.*, pages 381–475. Birkhäuser, Basel, 1999.
- [13] H. Hofer, K. Wysocki, and E. Zehnder. Finite energy cylinders of small area. *Ergodic Theory Dynam. Systems*, 22(5):1451–1486, 2002.
- [14] H. Hofer, K. Wysocki, and E. Zehnder. Finite energy foliations of tight three-spheres and Hamiltonian dynamics. *Ann. of Math. (2)*, 157(1):125–255, 2003.
- [15] U. Hryniewicz. Fast finite-energy planes in symplectizations and applications. *Trans. Amer. Math. Soc.*, 364(4):1859–1931, 2012.
- [16] U. Hryniewicz and P. A. S. Salomão. On the existence of disk-like global sections for Reeb flows on the tight 3-sphere. *Duke Math. J.*, 160(3):415–465, 2011.
- [17] U. L. Hryniewicz and P. A. S. Salomão. Elliptic bindings for dynamically convex Reeb flows on the real projective three-space. *Calc. Var. Partial Differential Equations*, 55(2):Art. 43, 57, 2016.
- [18] J. Kim and S. Kim. J^+ -like invariants of periodic orbits of the second kind in the restricted three-body problem. *J. Topol. Anal.*, 12(3):675–712, 2020.
- [19] S. Kim. Symmetric periodic orbits and invariant disk-like global surfaces of section on the three-sphere. *Trans. Amer. Math. Soc.*, 375(6):4107–4151, 2022.
- [20] W. S. Koon, M. W. Lo, J. E. Marsden, and S. D. Ross. Heteroclinic connections between periodic orbits and resonance transitions in celestial mechanics. *Chaos*, 10(2):427–469, 2000.
- [21] A. Liapounoff. *Problème Général de la Stabilité du Mouvement*. Annals of Mathematics Studies, No. 17. Princeton University Press, Princeton, N. J.; Oxford University Press, London, 1947.
- [22] D. McDuff and D. Salamon. *J-holomorphic curves and symplectic topology*, volume 52 of *American Mathematical Society Colloquium Publications*. American Mathematical Society, Providence, RI, 2004.
- [23] R. McGehee. *Some homoclinic orbits for the restricted three-body problem*. 1969. Thesis (Ph.D.)—The University of Wisconsin–Madison.
- [24] K. R. Meyer and D. C. Offin. *Introduction to Hamiltonian dynamical systems and the N-body problem*, volume 90 of *Applied Mathematical Sciences*. Springer, Cham, third edition, 2017.
- [25] J. Moser. Regularization of Kepler’s problem and the averaging method on a manifold. *Comm. Pure Appl. Math.*, 23:609–636, 1970.
- [26] P. A. S. Salomão. private communication. 2023.
- [27] R. Siefring. Intersection theory of punctured pseudoholomorphic curves. *Geom. Topol.*, 15(4):2351–2457, 2011.
- [28] C. Wendl. *Finite energy foliations and surgery on transverse links*. ProQuest LLC, Ann Arbor, MI, 2005. Thesis (Ph.D.)—New York University.

DEPARTMENT OF MATHEMATICS EDUCATION, KONGJU NATIONAL UNIVERSITY, KONGJU 32588,
REPUBLIC OF KOREA

Email address: seongchankim@kongju.ac.kr